Funded by the European Union

Horizon Europe Programme

HORIZON-WIDERA-2021-ACCESS-03

TWINN2SET

TWINNING TO SUSTAINABLE ENERGY TRANSITION

WP4: TWINN2SET RESEARCH PART

DELIVERABLE 4.2

Version 1.0

Task 1 - Reactivity and interactions between H_2 and microorganisms

Task 2 & 3 - Numerical simulations and thermodynamic aspects of H_2 storage in porous media

GRANT AGREEMENT 101079246
STATUS: FINAL
PUBLIC

Funded by the European Union

FORTH INSTITUTE OF GEOENERGY

Universitetet i Stavanger

IFP Energies nouvelles

Funded by the European Union. Views and opinions expressed are however those of the authors only and do not necessarily reflect those of the European Union. Neither the European Union nor the granting authority can be held responsible for them

Task 1: Elpida Maragkozoglou[3], Dr. Simon Poirier[1] & Dr. Elodie Muller[1]

Task 2: Efsevia Fragkou[3], Evina Gontikaki[3], Spyros Bellas[3], Emmanuel Stamatakis[3]

Task 3: Raoof Gholami[2]

[1] IFPEN Energies Nouvelles, France

[2] University of Stavanger, Norway

[3] Institute of Geoenergy/FORTH, Greece

Author printed in bold is the contact person/corresponding author

HISTORY OF CHANGES

Version Number	Publication Date	Brief Description of changes
1.0	21.05.2025	First version

TABLE OF CONTENT

I. INTRODUCTION & OBJECTIVES

The "Climate change" phenomenon has taken on rather large dimensions culminating in the "Paris agreement" in 2015. One of the main goals of this agreement was to reach net zero emissions by 2050 (Unfccc, 2015). Energy consumption is steadily increasing and consequently the use of carbon (C) based energy sources constitutes a global concern. The Energy Outlook of 2023 highlighted that the four main aims of the global energy's future are the declining role of hydrocarbons, the rapid expansion in renewable energies, the increase of electrification, and the growing use of low-carbon hydrogen (bp, 2023). The low-carbon hydrogen field is dominated by green hydrogen, produced by electrolysis using renewable power, and blue hydrogen, produced by natural gas or coal in combination with Carbon Capture and Storage (Heinemann *et al.*, 2021). During periods of renewable energy shortage, green hydrogen could be produced from the excess of renewable energy ("Power-to-Gas"), stored, and recovered when electricity generation is needed ("Gas-to-Power"). In this way, the imbalance between supply and demand, that withheld the renewable energy's dominance over the other energy sources, can be surpassed (Dopffel *et al.*, 2023; Thaysen *et al.*, 2023). Green hydrogen is a very promising fossil fuel substitute, which is expected to embody 60% of low-carbon hydrogen by 2030 (bp, 2023).

Hydrogen has high energy density since its gravimetric energy content is higher (140 MJ/kg) than hydrocarbons, for example natural gas (54 MJ/kg) (Dopffel, Jansen and Gerritse, 2021). However, its low density (0.084 kg/m3 at 20 °C and 0.1 MPa) necessitates the use of larger volumetric capacity reservoirs for its storage in comparison to natural gas when attempting to produce the same amount of energy (Heinemann *et al.*, 2021). The above ground hydrogen storage structures are well developed but their storage capacity and discharge times are limited. The underground storage reservoirs are an economical and feasible storage option for hydrogen (Thaysen *et al.*, 2023). As a liquid, hydrogen has a critical temperature of -239.97 °C and critical pressure of 1.297 MPa, and consequently it is stored in the gaseous phase. At geological storage conditions, hydrogen does not form hydrates but is almost three times more heat conductive than CH_4 and CO_2. The non-polar nature of hydrogen limits its solubility in water, which increases proportionally to pressure, as well as its density. Generally, there are some characteristics of hydrogen that must be considered for its storage procedure. Firstly, hydrogen has different physical and chemical properties than the gases which are usually stored. It can react with subsurface minerals and fluids, and it might trigger hydrogen consuming microorganisms' growth. Secondly, after repeated injection-recovery cycles, a change in the stress field in the storage site and a contamination might occur (Heinemann *et al.*, 2021).

Gases can be stored in surface storage facilities, like pipelines or tanks, or subsurface storage sites like depleted reservoirs, caverns, or deep aquifers (Heinemann *et al.*, 2021). The most feasible option for large-scale hydrogen storage is the underground storage in geological formations. These reservoirs are considered unaffected from fire, safe from extreme weather conditions, military actions, or terrorist attacks. They have great storage capacity. Their operational and investment costs are lower than the above ground storage reservoirs and the suitable geological storage sites are numerous (Dopffel, Jansen and Gerritse, 2021). The underground gas storage sites (UGSs) can be categorized regarding either their storage mode or their geological and hydrodynamic features, which are the most common. UGSs according to their features are divided to the porous types and to the non-porous types. The porous type UGSs consist of depleted oil and gas reservoirs, and deep aquifers. Artificial caverns and hard rock caverns belong to the non-porous types UGSs. Other specific and rare solutions are the lined and unlined hard rock storage and abandoned mines (Molíková *et al.*, 2022).

Depleted oil and gas reservoirs are the most common UGSs. They are economically feasible and well-documented. Their operation is possible by one to maximum two cycles of injection and withdrawal per year. The characteristics that must be taken into consideration are the shape, size and properties of the reservoir, the size of the aquifer layer, the gas-liquid phase, and the properties of the surrounding rock. The most important physical parameters at storage sites are porosity, permeability, and water saturation. Moreover, deep aquifers are defined by a porous rock layer with a proper anticlinal or adequate shape and suitable petrophysical parameters, filled with water at a certain depth. They have similar physical parameters to depleted reservoirs, that is porosity, permeability, formation pressure and sufficient capacity. However, they require a thorough geological investigation and greater investment. The gas injection and withdrawal take place once or twice a year (Molíková *et al.*, 2022).

The safety implications of hydrogen storage differ from the storage of other gases since the environmental risks are limited. Pure hydrogen is non-toxic, non-poisonous, non-corrosive, and environmentally friendly. However, gas leakage from a storage reservoir is a concern from a health, safety, economic and environmental perspective anyway (Heinemann *et al.*, 2021). The main and obvious safety concern regarding hydrogen gas leakage from a storage site is the explosion-associated risk of hydrogen release (Dopffel, Jansen and Gerritse, 2021). A monitoring system is necessary at a storage site in order to ensure the safety of injection-withdrawal operations and the possible leakage pathways, to inspect the mitigation of the gas in the subsurface, surveille the brine displacement due to pressure increase, and reassure the long-term safety of the storage site (Heinemann *et al.*, 2021).

Underground reservoirs harbor microbial ecosystems defined as SLiMEs (Subsurface Lithoautotrophic Microbial Ecosystems) (Haddad *et al.*, 2022). They consist of various populations that can notably depend on hydrogen and carbon dioxide as energy and carbon sources respectively. Subsurface microorganisms can also utilize energy sources in the surrounding rock or in dissolved components. The microbial community interacts with the reservoir's porous environment, since its rocks provide large surface area for biofilm formation (Dohrmann and Krüger, 2023a). In an environment consisting of intact rocks, microbial activity is 8-10 times higher than in a bulk environment (Khajooie *et al.*, 2024). Biofilm formation in the porous media and in the near-well regions or mineral precipitation may reduce hydrogen injectivity, since pore-clogging is more likely to happen, and change the transport properties of the subsurface (Heinemann *et al.*, 2021; Liu *et al.*, 2023). Hydrogen storage does not affect only the H_2-metabolizing microorganisms but also the syntrophic relationships in the microbial community (Dohrmann and Krüger, 2023a). However, if a reduction of the microbial diversity occurs, the risk of microbial consumption of hydrogen will not necessarily decrease (Dopffel, Jansen and Gerritse, 2021). The parameters that determine the interaction between the microbes and the rock after the injection/withdrawal of hydrogen from storage sites are the presence of carbon, temperature, salinity, pH, pressure, and the geological properties along with the site-specific microbial community (Thaysen *et al.*, 2023).

The microbes in the subsurface can have two possible origins. They either are indigenous, and were transported naturally and maybe via sedimentation processes, or they were anthropogenically introduced by human activity in the subsurface like drilling or mining. The latter complicates even more the study of these communities (Heinemann *et al.*, 2021). The alterations in microbial communities associated with hydrogen gas-storage can be sustained for several decades, and that is an important reason for their further investigation (Ranchou-Peyruse *et al.*, 2019).

Hydrogenotrophic microorganisms in the underground reservoirs convert hydrogen in products like acetate, CH_4 or H_2S (Heinemann *et al.*, 2021) that alter the habitat's conditions (Dohrmann and

Krüger, 2023a; Liu *et al.*, 2023). The four main groups of microbes that dictate the underground hydrogen storage reservoirs are the acetogens, sulfur species-reducing microorganisms (SSRM), the methanogens and dissimilatory iron reducing bacteria (DIRB). The first mainly alter the formation waters composition and pH, while the SSRM and methanogens impact the gas compounds present in the reservoir (Strobel, Hagemann, *et al.*, 2023). Growth of acetogens follows equation (1). Acetogens inhabiting horizons of underground gas reservoirs are usually responsible for organic acids found in water samples (Nazina *et al.*, 2023). These organic acids lead to a pH drop of the UGSs' water repositories, which can be the products of these microorganisms' growth on hydrogen and CO_2 (Tarasov *et al.*, 2011).

$$4H_2 + 2HCO_3^- + 2H^+ \Rightarrow C_2H_4O_2 + 4H_2O \quad (1)$$

SSRMs are very common, and they include various microbial groups potentially using hydrogen as electron donor when sulphate is present as electron acceptor. The reaction between hydrogen and sulphate is described by the chemical equation (2). The product of this reaction is a toxic and corrosive gas, H_2S. The surrounding pH usually increases because it is a proton consuming process (Dopffel *et al.*, 2023). The reaction of sulphate reduction is very efficient and low amounts of sulphate may lead to a great amount of H_2S (Dopffel, Jansen and Gerritse, 2021).

$$4H_2 + SO_4^{2-} + 2H^+ \Rightarrow H_2S + 4H_2O \quad (2)$$

Another highly relevant consumer group of hydrogen is hydrogenotrophic methanogens. In methanogenesis, both hydrogen and carbon dioxide are consumed and lead to methane production and pH increase, as depicted in equation (3). Bio-methanation is a topic rapidly gaining interest because it is believed that methane constitutes an improvement to the calorific value of the stored gas (Strobel, Zawallich, *et al.*, 2023). However, when methanogenesis is combined with the deterioration of the greenhouse balance, the loss of hydrogen must be considered as a hydrogen storage risk (Heinemann *et al.*, 2021; Dopffel *et al.*, 2023).

$$4H_2 + HCO_3^- + H^+ \Rightarrow CH_4 + 3H_2O \quad (3)$$

The SSRM and methanogens are usually the most abundant microorganisms in the UGSs. However, in habitats where iron and organic carbon are in surplus and regardless of the environmental conditions, the DIRB dominate over other hydrogenotrophs because of their high affinity for hydrogen (Thaysen *et al.*, 2023). Growth of DIRB follows the equation 4.

$$2FeOOH + H_2 + 4H^+ \Rightarrow 2Fe^{2+} + 4H_2O \quad (4)$$

The 16s rRNA gene sequence is used to monitor all these microorganisms. This sequence is a valuable and irreplaceable marker because of its evolutionary rigidity. It is usually considered as a living fossil carrying information about the origin of the domains of cellular life. However, 16s rRNA gene is not a species-specific marker since its applicability beyond the genus level is highly limited (Bartoš, Chmel and Swierczková, 2024). The quantification of the population of certain groups of microorganisms is based on more specific phylogenetic markers. Representative examples are the *dsrB* gene, which encodes the dissimilatory sulfite reductase β sub-unit, and the *mcrA*, which encodes

a sub-unit of the methyl-coenzyme M reductase I, which have been used for SSRM and methanogens respectively (Ranchou-Peyruse *et al.*, 2019).

In order to achieve absolute control over hydrogen reservoirs there are certain knowledge gaps that need to be filled. Firstly, there is a lack of microbial data from field tests especially considering the variety of microbial population that exist in these storage sites. The effects on these microbial communities of the high concentration and partial pressure of hydrogen are also unexamined. Further research must occur regarding the effects of hydrogen leaks on groundwater chemistry and microbiology, but also the relation between microbiological activity and geochemical parameters. Microbial mitigation methods are also an important field of research, besides the broad-range biocides or metabolic inhibitors (Dopffel, Jansen and Gerritse, 2021). However, biocides are a temporary solution and may enhance corrosion risks. Another possible solution and field of research is the selection of an appropriate hydrogen storage site. The choice must be based on the physicochemical growth constraints of the main hydrogenotrophs and thus restrict the microbial effects on the storage site, the hydrogen loss, and the gas contamination (Thaysen *et al.*, 2023).

In this context, the objective of the internship of Elpida Maragozoglou was to conduct a sensitivity analysis on environmental parameters influencing H_2 consumption by a hydrogenotrophic methanogen strain. To complement these data, the possible consumption of H_2 by an environmental microbiome sampled from an aquifer prior to H_2 injection was characterized as part of the ANR HyStorEn project. These two sets of data are presented hereafter.

II. MATERIAL & METHODS

1. Experimental set-up

A. Culture conditions

Culture medium DSMZ 814 was composed of NaCl (0.45 g/L), $MgCl_2$•$6H_2O$ (0.03 g/L), NH_4Cl (0.4 g/L), $FeSO_4$•$7H_2O$ (0.1, w/v in H_2SO_4), and KH_2PO_4 (0.5 g/L) and 1 g/L of tryptone. The medium was supplemented with 10 mL of a modified mineral solution of Wolin and 1 mL of vitamin solution **Table 1**. After filtration at 0.22 µm, the pH was adjusted at 8.0-8.5 with a potassium hydroxide solution (3 M). As an indicator of the reducing capacity of the prepared medium, 0.52 v/v of sodium resazurin (250 mg/L) was used. For the transitions to anaerobic conditions, the medium was flushed with N_2 for 40 min. The medium was enriched with L-cysteine and Na_2CO_3 at final concentrations of 0.25 g/L and 1 g/L, respectively. It was then reduced with sodium sulphide (Na_2S, $9H_2O$) from a sterile stock solution, at a desired final concentration of 0.25 g/L. The medium was distributed in anaerobic flasks of 150 mL. The volume of the liquid phase in each flask was 50mL. Headspaces were flushed three times and pressurized (1 bars at 20 °C) with H2/CO2 (75/25, v/v).

Table 1. Wolin's modified mineral solution and vitamin solution ingredients.

Modified mineral solution of Wolin			**Vitamin solution**		
		g/L			g/L
Nitrilotriacetic acid	NTA	1.5	Cobalamin	B12	0.1
pH adjustment at 6.5 with 3M KOH solution			p-Aminobenzoic acid	B10	0.08
Magnesium sulphate	$MgSO_4$•$7H_2O$	3.0	D- (+)-biotin	B7	0.02
Manganese sulphate	$MnSO_4$•H_2O	0.5	Nicotinic acid	B3	0.2

Sodium Chloride	NaCl	1	Calcium pantothenate	B5	0.1
Ferrous sulphate	$FeSO_4•7H_2O$	0.1	Pyridoxine hydrochloride	B6	0.3
Cobalt sulphate	$CoSO_4•7H_2O$	0.18	Thiamine-HCl-$2H_2O$	B1	0.2
Calcium chloride	$CaCl_2•2H_2O$	0.1			
Sulphate de zinc	$ZnSO_4•7H_2O$	0.18			
Copper sulphate	$CuSO_4•5H_2O$	0.01			
Potassium alum	$AIK(SO_4)_2•12H_2O$	0.02			
Boric acid	H_3BO_3	0.01			
Sodium molybdate	$Na_3MoO_4•2H_2O$	0.01			
Nickel Chloride	$NiCl_2•6H_2O$	0.03			
Sodium Selenite	$Na_2SeO_3•5H_2O$	100 mL (3g/L)			
Sodium tungstate	$Na_2WO_4•2H_2O$	100 mL (4g/L)			
pH adjustment at 7.0 with 3M KOH solution					

B. Source of organisms

Methanobacterium formicicum DSMZ 1535 (MFO) was selected as the microorganism for the pure culture kinetic and parametric studies because it is a well-known methanogenic microorganism. For each experiment, a cryotube stored at -80°C was used as the inoculum for their preculture.

The environmental consortium was sampled in Saint Emilion (France) from an aquifer as part of the ANR Hystoren project. A total volume of 2 L was collected and filtered through a 0.22 µm filter to concentrate the microbial populations. This filter was incubated in agitated conditions (110 rpm) at 30°C for one week. Once more than 90% of the total H_2 was consumed, 1 mL was transferred to a second flask in the same conditions in order to select the active hydrogenotrophic populations.

This anaerobic consortium was specialized in flasks with the standard culture medium (see above) and under H_2/CO_2 (75:25, v/v) during several months prior to the experiments to select the hydrogenotrophic metabolisms that may interact with gas storage in deep environments (e.g., methanogenesis, sulphate reduction, homo-acetogenesis). The inoculum (1 mL) was derived from the liquid sample from the underground cavities in Saint-Emilion, which was incubated in the lab at 30°C with H_2/CO_2 (75:25; v/v; 1 bar) as the gas phase.

C. H_2 consumption kinetics

Sensitivity of *M. formicicum* H_2 consumption kinetics was examined under the parameters of salinity, and temperature and salinity combined. The parameters tested are listed at **Table 2**. All the parameters were tested in triplicates.

Table 2. The sensitivity of M. formicicum H_2 consumption kinetics was tested under the parameters of salinity, temperature, and the combination of them.

Parameters studied	
Salinity (M)	0, 0.5, 0.75, 1
Temperature (°C)	30, 37, 42

H_2 consumption kinetics of the environmental consortium were monitored as detailed below. After the end of each kinetic, a new experiment was initiated using an inoculum from the previous one. This procedure was repeated twice. The experiments were carried out in agitated conditions (110 rpm) until complete consumption of H_2 and/or CO_2 from the headspace gas. All incubations were performed in triplicates. Abiotic control experiments were also conducted at each temperature to identify any alterations between the gas phase and the medium. Thereby, variations of the pressure, and the aqueous and gas phase composition were measured at time zero (T0) and twice every day.

2. Microbial activity analyses

A. Measurements

During the incubation, pressure measurements and gas analysis were performed at regular time points. The variations at the pressure measurements were measured using a differential manometer (Digitron 2082P) before and after each sampling session. When the pressure was about 50% reduced, the samples were repressurized with N_2. Gas analysis was carried out by micro gas chromatography (Micro GC Fusion, Inficon). The composition of the different gases of the headspace (in %) was used to calculate their respective amounts applying the ideal gas law:

$$n = PV/RT \qquad (1)$$

where 'n' is the amount of gas [mol], 'P' is pressure [Pa], 'V' is the volume of headspace taken by the respective gas [m^3], 'R' is the gas constant 8.314 462 [J/mol K], and 'T' is temperature [K].

B. Sampling

Liquid samples were taken after gas analysis. During the liquid sampling procedure 1 mL was collected through the septum under continuous N_2 flow. The liquid samples were then photometered at 600 nm using a Benchtop Spectrophotometer for Water Analysis (DR3900, HACH LANGE), to estimate the growth of the culture. pH was measured with SevenEasy™ pH meter (METTLER TOLEDO). The samples were centrifuged at 14000 x g, and the pellets and supernatants obtained were stored separately at −20 °C for DNA and chemical indicators analysis respectively.

3. Molecular analyses of microbial communities

A. DNA extraction and PCR amplification

DNA-based analysis was performed at the liquid samples of the consortium for several time points at the three different kinetic analyses that were conducted. The total DNA was extracted from the pellet using the DNeasy Powersoil Pro kit (QIAGEN) according to the manufacturer's instructions. The concentration of the extracted DNA was quantified using a fluorescent dye assay (Qubit dsDNA HS Assay Kit, Invitrogen, Eugene) and Qubit 2.0 Fluorometer (Invitrogen, Life Technologies, Eugene). Pending their sequencing the samples were stored at -20°C. For the characterization of bacterial communities, the V3-V4 region of 16S rRNA gene was targeted (≈450 bp). For the characterization of the fungal ones the ITS region was targeted (the highly variable ITS1 subregion). Two rounds of amplification were performed by Eurofins Genomics to construct the amplicons libraries. The primers used for the PCRs are presented in **Table 3**. Sequencing was performed using Illumina technologies, MiSeq V3 (read mode 2x300 bp).

Table 3. Primers designed for the DNA-sequencing analysis.

Primers

Bacteria	5'-3'	V3	CCTACGGGNGGCWGCAG
	5'-3'	V4	GGATTAGATACCCTGG
Fungi	5'-3'	ITS1	GGAAGTAAAAGTCGTAACAAGG
	5'-3'	ITS1	GCATCGATGAAGAACGCAGC

B. Metagenetic sequence analysis

Eurofins Genomics provided the quality control and the sequence merging metrics of the sequenced amplicons. For retaining the high-quality bases by performing adapter trimming, quality filtering and per-read quality pruning the quality control of raw sequences is necessary. Data were analyzed in the Galaxy platform and imported into the FROGS (Find Rapidly OTUs with Galaxy Solution) pipeline (Escudié *et al.*, 2018). Using this pipeline, the sequence reads are demultiplexed, clusters are created, chimeras are removed, and an OTU taxonomic affiliation is generated. It also provides a great number of filters regarding the clusters that will be created and the affiliation that will be reported so the result can be as precise as possible. The databases used for the taxonomic affiliation as a reference database were 16S EZBioCloud (release 52018) (Yoon *et al.*, 2017) and UNITE Fungi 9.0 (UNITE).

III. RESULTS

1. Methanobacterium formicicum

A. H_2 consumption dynamics

Methanobacterium formicicum (DSMZ 1535) consumes H_2 and CO_2 concomitantly. Several parameters that can influence this consumption were tested and the maximum H_2-consumption rate for each parameter were calculated. Control incubations were performed without the presence of the microorganism so the different dilution rates between gas-phase and liquid-phase during the incubation will be monitored.

a. Evidencing the optimum pH for H_2-consumption

M. formicicum's H_2-consumption and CH_4-production kinetics were tested under different pH values (7, 7.5, 8.5, 9) at 37°C (**Figure 1**). The pH was adjusted at these values after the addition of 1 bar H_2/CO_2 (75:25, v/v) in the gas-phase. The pH 7 presented the most rapid H_2-consumption rate by consuming 5074 ± 13 µmol in two days and the highest quantity of produced CH_4, 1742 ± 51 µmol. However, by increasing the pH to 7.5 the H_2-consumption was greatly affected. Firstly, the consumption started to slow down after the second day of monitoring and eventually it was never fully consumed since 148 ± 54 µmol remained in the gas-phase. Additionally, the produced methane was ≈26% lower at pH 7.5 than at pH 7, since the final quantity was 1165 ± 25 µmol. Activity was observed at pH 8.5, but both the H_2-consumption and the CH_4-production were severely lower compared to the pH 7. The amount of 3011 ± 89 µmol of hydrogen remained in the gas-phase after the eight-days period and only 342 ± 52 µmol of methane was produced. At pH 9 *M. formicicum* consumed only a very low quantity of hydrogen, 521 µmol, and consequently it produced a similarly low quantity of methane, 53 ± 10 µmol.

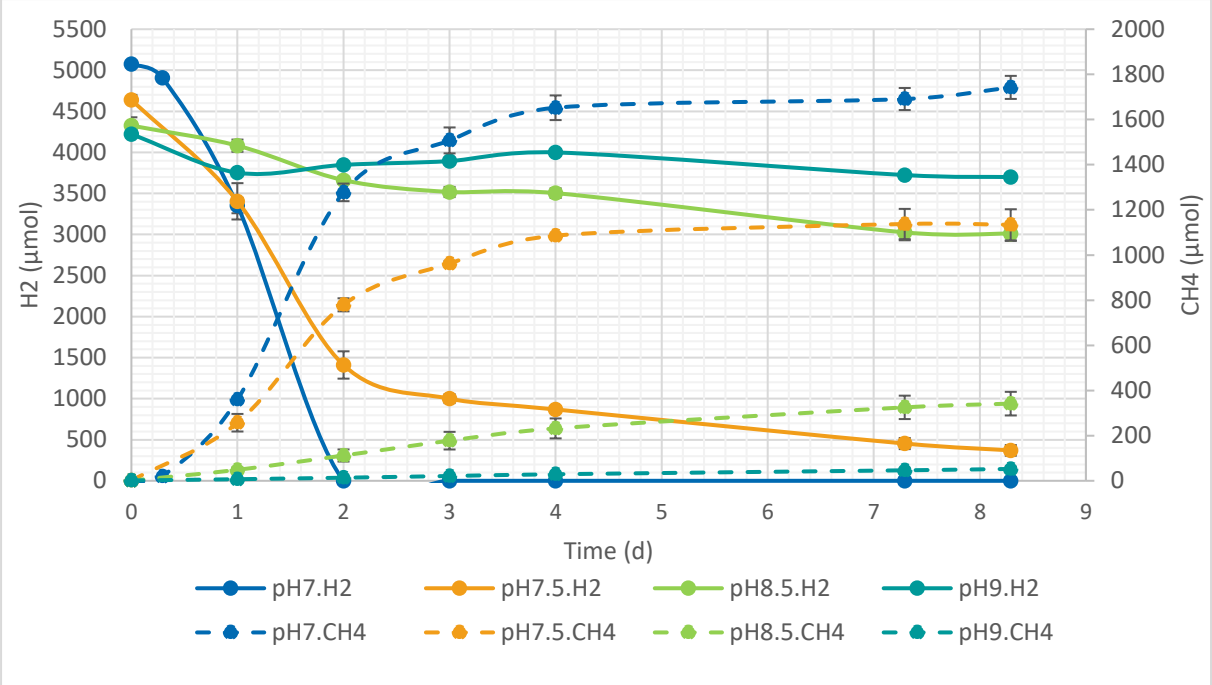

Figure 1. Kinetics of M. formicicum at different pH.

The microbial growth of *M. formicicum* was decreasing while the pH was increasing, as depicted at **Table 4**. The ΔOD_{600} observed at pH 7 was +0.205, while at pH 7.5, 8.5, and 9 was +0.151, +0.075, and +0.034 respectively. Some growth was observed in all the different pH conditions. On the contrary an alkalinization was not noted at every pH value. At pH 7 the pH of the culture was increased by 1.34. However, the highest increase was 1.66 and it was noted at the pH 7.5 cultures. At pH 8.5 the pH increased only by 0.53, while at pH 9 there was any increase at the pH of the culture. The highest alkalinization took place at pH 7.5, but it did not differ greatly from the one observed at the optimum pH.

Table 4. Growth variation of M. formicicum and pH alteration of the cultures under different pH values. The measurements at pH 7 are mentioned for comparison purposes.

Samples	**OD600**		**pH**	
pH	ODmax	**ΔOD600**	pHmax	**ΔpH**
7	0.236	+0.205	8.45	+1.34
7.5	0.154	+0.151	9.32	+1.66
8.5	0.096	+0.075	9.06	+0.53
9	0.048	+0.034	9.12	-0.02

The maximum hydrogen-consumption rate was calculated for various pH values, too. The R_{max} at pH 7 was equal to 3352 µmol/day. The R_{max} at pH 7.5 was lower than the one at the pH 7 since it was equal to 1993 µmol/day. Furthermore, the R_{max} at pH 8.5 and 9 was 625 and 637 µmol/day respectively. These values indicate that there is a small activity of *M. formicicum* at these two high pH conditions. Consequently, based on the H_2-consumption, the CH_4-production, and the microbial growth the optimum pH of *M. formicicum* is pH 7.

b. Influence of temperature and salinity at H_2-consumption

- **Gas-phase analyses**

The ability of *M. formicicum* to consume hydrogen was tested in four different salinity concentrations under three different temperatures, 30, 37, and 42 °C. The initial difference of the H_2 quantity between the three kinetics is due to the subsequent subtraction of the H_2-amount consumed by the analysis from the total H_2-amount at each measurement of the culture's gas-phase. For example, at 30 °C the kinetic study lasted for more days than the other two and more samples both gaseous and liquid have been taken, and more quantity of hydrogen have been consumed by the analysis. That is the reason why the initial quantity of hydrogen appears lower than at the other two temperatures, even if all cultures started with the same quantity and concentration of gas-phase. The H_2-consumption is depicted at **Figure 2**. At 0M NaCl salinity, hydrogen was fully consumed in 3 days at 37 °C, in 4 days at 30 °C, and at 42 °C in 7 days. The kinetics of H_2-consumption at 30 and at 37°C present a lot of similarities. They both start with a lag phase of 1.3 days and are complete before the fourth day. At 37°C, 5139 ± 46 μmol of H_2 were consumed in 3 days, while at 30°C 4072 ± 238 μmol were consumed in 4 days. The kinetics at 42°C present a different profile since there is no lag phase and the consumption of hydrogen slows down after the fourth day since only 248 μmol were consumed from the morning measurement until the afternoon one on that day. Additionally, the total amount of hydrogen was consumed by the seventh day. At a low concentration of NaCl (0.5M), H_2-consumption at 37°C was completed with a delay of one day but it was completed on the same day, the seventh one, at 30 and 42°C. At 37°C the consumption presents a similar lag phase with 0M and 0.5M NaCl of 1.3 days, but at the second salinity condition the microorganism needed 4 days to consume 4661 ± 39 μmol of hydrogen. Additionally, at 0.5M NaCl the profile of the consumption is similar either at the lower temperature, 30°C, or the highest one, 42°C because there was a consumption of 2645 ± 278 and 5138 ± 124 μmol respectively within 7 days. At 0.75M NaCl a H_2-consumption of 2037 μmol occurs at 42°C, but not at the other two temperatures. Finally, at the highest salinity concentration, 1M NaCl, there is no consumption at any temperature. It appears that the consumption of hydrogen is affected differently when the parameters of salinity and temperature are combined. The presence of salts aids the H_2-consumption activity of *M. formicicum* at higher temperatures and vice versa.

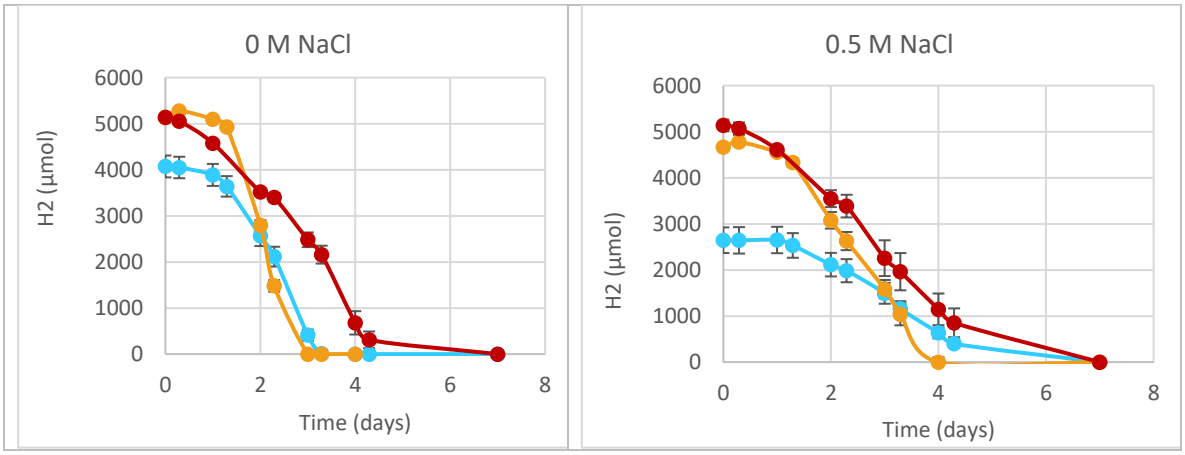

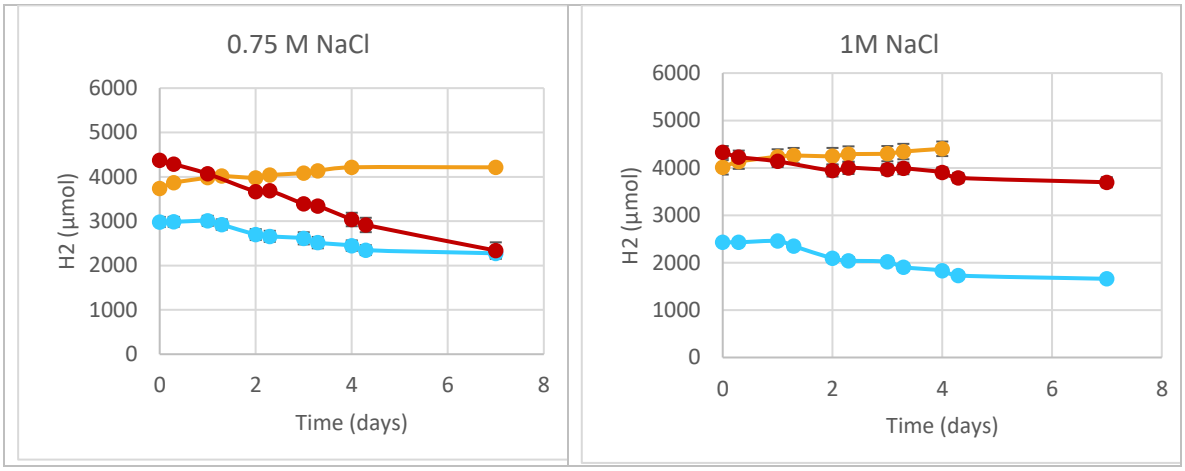

Figure 2. H_2-consumption of M. formicicum at a double-parametric study. The red line is the H_2-consumption at 42°C, the orange at 37°C, and the lite blue for the 30°C.

The maximum consumption rate (R_{max}) of hydrogen was calculated for all the different parameters studied, which are presented at **Table 5**. At 37°C it was more than twice higher at 0M NaCl concentration than at 0.5M, since R_{max} was equal to 4515 and 1867 μmol/day respectively. Among the different temperatures the highest consumption of hydrogen was noted at 37°C. Nevertheless, the consumption at 30°C and 42°C did not present a great difference. The R_{max} at 0M was equal to 2405, 4515, and 2089 μmol/day at 30°C, 37°C, and 42°C respectively. Thus, the hydrogen consumption decreased by ≈46% at 30°C and ≈54% at 42°C.

Table 5. Maximum hydrogen consumption of Methanobacterium formicicum.

	R_{max} (μmol/day)		
[NaCl]	30°C	37°C	42°C
0M	2405.30	4514.75	2089.30
0,5M	1146.37	1866.68	1594.86
0,75M	344.81	445.75	429.10
1M	388.02	406.07	397.59

Moreover, at 30°C as the concentration of salts was increasing the R_{max} was decreasing. At 0.5M R_{max} was equal to 1146 μmol/day and its value dropped at 345, and 388 μmol/day at 0.75M and 1M concentrations respectively. At 42°C and with a 0.5M NaCl concentration the R_{max} was similar with the one presented in the same salinity at the optimal temperature (37°C), since R_{max}=1595 μmol/day and R_{maxopt}=1867 μmol/day. The R_{max} at 0.75M and 1M NaCl were again lowered since they were equal to 429 μmol/day and 398 μmol/day respectively. It appears that the maximum hydrogen consumption of *M. formicicum* in the presence of salts is improved at higher temperatures.

The consumption of carbon dioxide was also tested in the same conditions. The initial difference of the CO_2 quantity between the three kinetics is due to the subsequent subtraction of the CO_2-amount consumed by the analysis from the total CO_2-amount at each measurement of the culture's gas-phase similarly with the H_2-consumption kinetics. As depicted at **Figure 3** the kinetics of CO_2-consumption are concomitant with the H_2-consumption, which is expected since both gases were being consumed concomitantly. However, carbon dioxide was fully consumed at 0 and 0.5M NaCl at only 37 and 42°C. At 30°C only hydrogen was fully consumed since 125 ± 5 and 83 ± 3 μmol remained in the gas-phase at 0M and 0.5M NaCl respectively. At 0.75M NaCl, CO_2-consumption of 189 μmol occurred only at 42°C similarly with H_2. At 1M NaCl there was no consumption at any temperature tested. The increase in the quantity of CO_2 at the beginning of the kinetics is due to the CO_2-release

from the medium of the culture when the incubation starts, which is probably a result of temperature increase. This increase occurs similarly to all the samples since they had the same medium, initial pressure, and gas-composition at the beginning of this experiment.

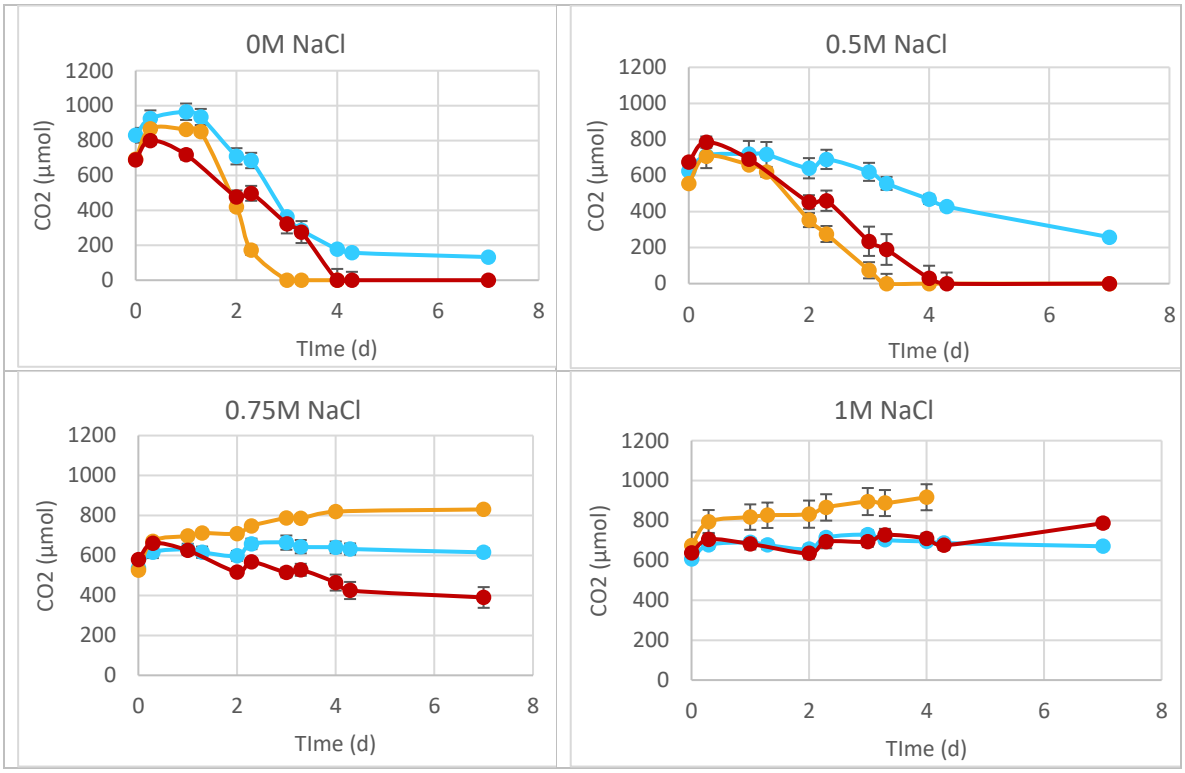

Figure 3. CO2-consumption of M. formicicum at a double-parametric study. The red line is the CO2-consumption at 42°C, the orange at 37°C, and the lite blue for the 30°C.

Furthermore, methane production was tested at the same conditions and the results are presented in **Figure 4**. The highest quantity of produced methane was observed at 37°C, 0M NaCl with a final value of 1571 ± 27 μmol. Additionally, at 37°C even if the hydrogen was fully consumed both at 0M and 0.5M NaCl, the final concentration of methane was not equal between the two conditions since it was equal to 1463 ± 33 μmol at the second one. At 0M NaCl, the CH_4-production was similar at 30 and 42°C, with a slightly higher quantity-value at the second one. The quantity of methane produced at 30°C was 1135 ± 86 μmol and at 42°C 1299 ± 21 μmol. At 0.5M NaCl the CH_4-production at 42 °C was equal to 1323 ± 40 μmol and it was almost the same with the one at 0M. On the contrary at 30°C it decreased at 560 ± 36 μmol. At 0.75M NaCl methane was produced only at 42°C and it was equal to 510 ±15 μmol. At 1M there was no production at any temperature. The production of methane is affected similarly with H_2-consumption at various salinity and temperature conditions. However, the fact that a certain quantity of hydrogen was consumed each time by the analysis must be taken into consideration. For example, the final amount of methane at 0M NaCl and 30 °C might be higher since a great quantity of hydrogen was consumed by the analysis.

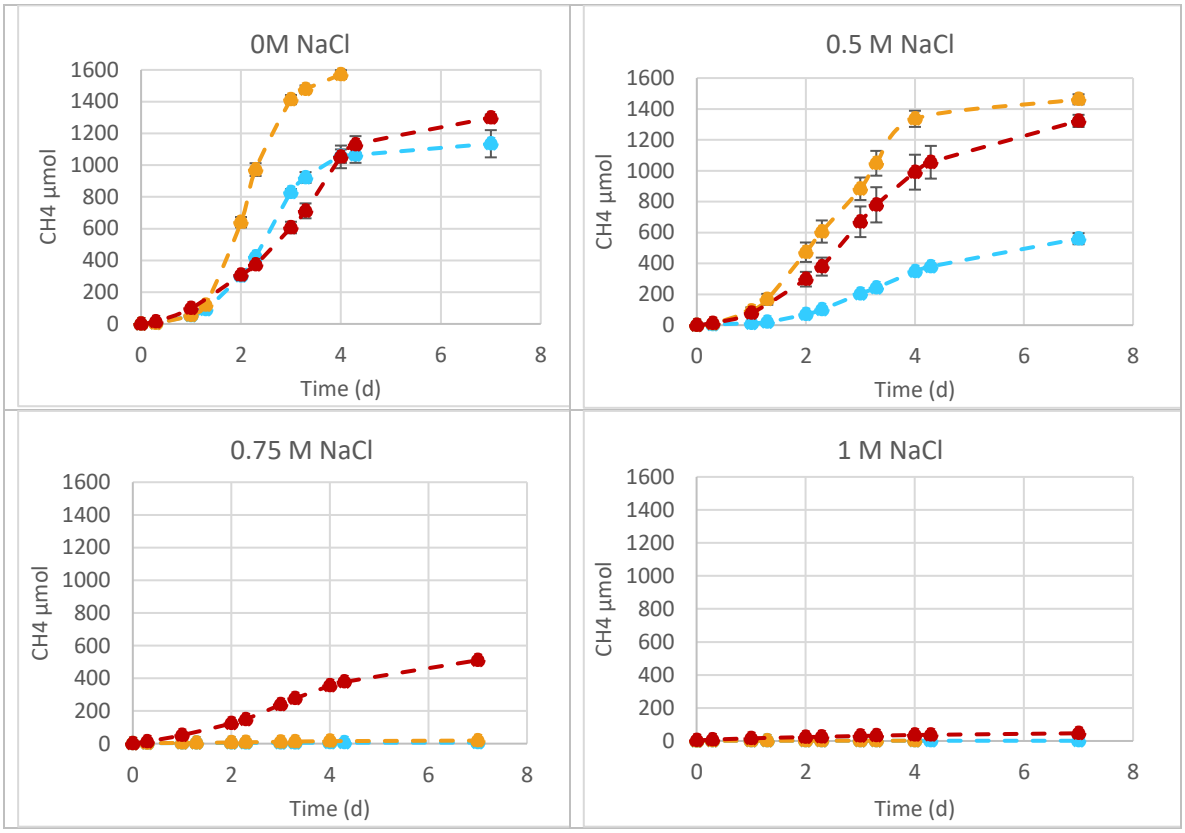

Figure 4. CH_4-production of M. formicicum at a double-parametric study. The red line is the CH_4-production at 42°C, the orange at 37°C, and the lite blue for the 30°C.

- **Liquid-phase analyses**

The microbial growth was monitored by measuring the optical density of the liquid samples, which is cited at **Table 6**. The highest growth was observed at 37°C and 0M NaCl as expected from the hydrogen and carbon dioxide-consumption kinetics. Additionally, at 37°C the ΔOD_{600} of the cultures with 0.5M NaCl was equal to +0.185 and it was ≈28% less than the one at 0M, +0.256, while at the higher salt concentrations, 0.75M and 1M, no growth occurred. At 30°C and 0M the growth of *M. formicicum* was similar to the growth at 37°C and 0M NaCl, since ΔOD_{600} was equal to +0.204, but it was lower at 0.5M with an increase of 0.083 at the optical density. At 42°C there was barely a growth at 0M concentration, because the ΔOD_{600} was only +0.086, even if there was consumption of hydrogen and production of methane. However, at 0.5M the growth is even greater than the one at 30°C, since the ΔOD_{600} was +0.132 but it does not reach the one at 37°C. Additionally, a very limited growth takes place at 42°C at 0.75M and 1M NaCl with ΔOD_{600} equal to +0.048 and +0.035 respectively. Regarding the pH alteration, at 37°C there was an almost equal alkalinization in both 0M and 0.5M cultures since the increase was 0.89 and 0.85 respectively. At the higher salinities, 0.75M and 1M NaCl, the pH alteration was not significant because it increased only by 0.09 and 0.10 respectively. Alkalinization was observed in all cultures with 0M NaCl salinity at 30 and 42°C, which was higher than the one observed at 37°C. At 30°C the pH-increase was 0.92 and 1.19 at 42°C. A pH-increase of 0.80, 0.31 and 0.35 was noted at 30°C at 0.5M, 0.75M and 1M NaCl respectively. However, at the salinities 0.75M and 1M NaCl there was no microbial growth. Finally, the highest alkalinization occurred at 42°C and 0.5 NaCl where the pH increased for 1.22 values.

Table 6. Growth variation of M. formicicum and pH alteration of the cultures at all the parameters studied.

Samples	OD600	pH

37°C				
	OD_{max}	**ΔOD600**	pH_{max}	**ΔpH**
0M	0.281	+0.256	7.90	+0.89
0.5M	0.217	+0.185	7.68	+0.85
0.75M	0.010	-0.022	6.88	+0.09
1M	0.010	-0.028	6.87	+0.10
30°C				
	OD_{max}	**ΔOD600**	pH_{max}	**ΔpH**
0M	0.227	+0.204	7.82	+0.92
0.5M	0.113	+0.083	7.53	+0.80
0.75M	0.022	-0.002	6.96	+0.31
1M	0.018	-0.014	6.97	+0.35
42°C				
	ODmax	**ΔOD600**	pH_{max}	**ΔpH**
0M	0.096	+0.086	8.26	+1.19
0.5M	0.154	+0.132	8.13	+1.22
0.75M	0.048	+0.034	7.23	+0.33
1M	0.035	+0.023	6.97	+0.16

2. Environmental sample

A. H_2 consumption dynamic

The environmental sample studied in the ANR HyStorEn project was an anaerobic microbial consortium that was also consuming both H_2 and CO_2. For the environmental sample this study was focused on the attempt to specialize the microbial community through a chained series of cultures. Each culture was the source of the inoculum for the next one. The kinetic growth and the hydrogen consumption of each culture were monitored, and the maximum H_2-consumption rate was calculated. Each step of this series of cultures was tested with triplicates.

The first culture of this series was “Con0” and theoretically was the one with the highest microbial diversity (**Figure 5**). Its kinetic growth was monitored for more than two weeks, and the hydrogen was never fully consumed. A quantity of 703 ± 108 µmol remained at the gas-phase. The lag phase lasted for one day and then the H_2-consumption occurred with a slow rate, since only 3789 µmol were consumed within 12 days. The second culture of the series was “Con1” and was inoculated from Con0. Con1 did not have a lag phase and hydrogen was never fully consumed, but a H_2-consumption of 4469 µmol within only 10 days was noted. The quantity of hydrogen decreased at ≈ 1400 µmol and remained stable for days. This amount of gas probably was the trapped gas in the top of the culture’s flask, which was not in contact with the culture’s medium and was due to the vertical agitation of the flasks during the incubation. The last culture of that chained series was “Con2” which presented a two-day period that could be considered as a lag time and a H_2-consumption equal to 3757 µmol which was similar to the one noted from Con0. Hydrogen was not fully consumed in this culture, too.

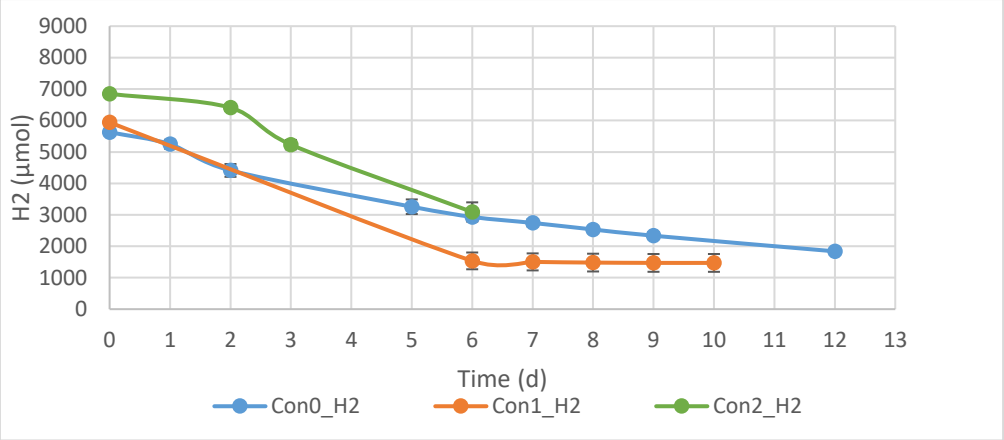

Figure 5. H_2-consumption by the three different cultures produced by an environmental consortium. In this graph it is not depicted the exact duration of each kinetic study. The Con0 culture was monitored for 23 days in total and Con1 for 17 days.

The product of the hydrogen and carbon dioxide consumption of this environmental consortium was H_2S. The amount of H_2S which was produced by the first culture, Con0, was equal to 50 ± 2 μmol. Both, Con1 and Con2 reached the same amount of hydrogen sulphide, which was equal to 38 ± 1 and 39 ± 2 μmol respectively.

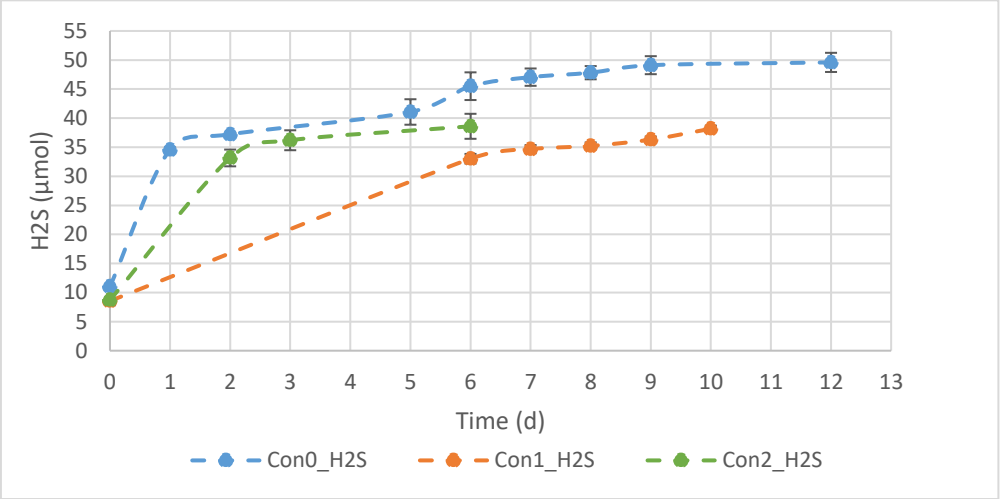

Figure 6. H_2S-production by the three different cultures produced by an environmental consortium. In this graph it is not depicted the exact duration of each kinetic study. The Con0 culture was monitored for 23 days in total and Con1 for 17 days.

The microbial growth rate of this series of cultures was increasing from one culture to another, as depicted in the following table (**Table 7**). More specifically, Con0 presents a ΔOD_{600} equal to +0.124, Con1 +0.215 and Con2 +0.272, which is the highest one. In addition, the pH of all the cultures decreased. The pH-decrease was equal to 0.42, 0.54, and 0.38 for Con0, Con1, and Con2 respectively. The CO_2-consumption usually leads to increase of the pH. In this case the only possible explanation is that there was production of acetate but since there was not any measurements regarding acetate in this study this is only an assumption.

Table 7. Growth variation and pH alteration of the environmental consortium.

Samples	OD600	pH

	ODmax	**Δ OD600**	tfinal	**ΔpH**
Con0	0.207	+0.124	6.50	-0.42
Con1	0.285	+0.215	6.30	-0.54
Con2	0.354	+0.272	6.28	-0.38

The maximum hydrogen-consumption rate was also calculated for these cultures. The R_{max} of the first culture was 834 μmol/day. However, the R_{max} of the second one, Con1, was lower than Con0's one, with a value equal to 734 μmol/day. The difference is not great but from the growth results the opposite situation was expected. The highest R_{max} was calculated for Con2 as expected, which was 1176 μmol/day. All the cultures were attempted to be revived but since the microorganisms at the end of each kinetic experiment were not active, this attempt was not successful. Hence, a substrate deprivation was confirmed since the microbial consortium was not able to enter a "dormant state" after the kinetic experimentation.

B. Monitoring of the sulphate-consumption

The presence of sulphate in the cultures was monitored with the liquid samples derived from the cultures of the kinetic analysis of this consortium. Sulphate is the substrate that is usually transformed to H_2S, so the percentages of their consumption and production respectively will be opposed. The sulphate concentration at the first sample of the Con0 was 74.83 mg/L and at the last one was 62.67 mg/L. Thus, at the first culture there was a 16.3% reduction of sulphate, which led to a 78.6% production of hydrogen sulphide. At Con1 culture the sulphate concentrations were 73.67 and 62.00 mg/L at the first and the last sample respectively. There was a 15.8% consumption of sulphate and a 77.6% production of H_2S, which are similar values with Con0. At Con2 culture the sulphate concentration at the first sample was 73.67 mg/L and at the last 69.50 mg/L. The consumption of sulphate at Con2 culture was 5.7% and the production of H_2S was 77.4%. The consumption of sulphate is a lot lower than the other two cultures, although the percentages of hydrogen sulphide production of the three cultures are very similar. These measurements and calculations are cited in the following table (**Table 8**).

Table 8. The percentages of sulphate-consumption and hydrogen sulphide-production.

	Sulphate (mg/l)			**Hydrogen sulphide (μmol)**		
Samples	t0	tfinal	**Reduction** (%)	t0	tfinal	**Production** (%)
Con0	74.83	62.67	-16.3%	11.04	51.54	+78.6%
Con1	73.67	62.00	-15.8%	8.55	38.17	+77.6%
Con2	73.67	69.50	-5.7%	8.71	38.60	+77.4%

C. DNA-based microbial community analyses of an environmental sample

A 16S-rRNA high-throughput sequencing was performed on three liquid samples in triplicates to analyze the microbial communities dynamic in the chained series of cultures and identify the key microorganisms potentially involved in H_2-consumption. For bacteria between 66563 to 93284 sequences were identified and assembled into 49 OTUs. In all samples *Terrisporobacteur*

petrolearius was 100% identified with a relative abundance of more than 50% of the bacterial population. The presence of this bacterium seemed to increase in the consortium from the first culture to the second one. There was another species that was 100% identified, *Clostridium huakuii*, with an average value of relative abundance equal with 21%. This species' presence appeared stable in the entire chained series of cultures. A multi-affiliated sequence was found with an abundance of 13-23%. Most of the species identified with this sequence belonged to the *Aeromonas sp.*, with *Aeromonas hydrophila* being the most popular candidate. This species is an anaerobic bacterium which can reduce sulphite to H_2S. Some high-abundant sequences were found in different percentages in the cultures, or only in some of them. This indicates that the microbial community was altered between the different fermentation cycles. More specifically, a multi-affiliated sequence appeared with a 0.9-1.5% abundance in the first two cultures and with 2-3.5% one in the third one. This sequence presents a 96.52% homology with one in the *Clostridium thailandense* species. It does not appear in any other identified species. In the first culture another multi-affiliated sequence is present but then it disappears in the following ones. This sequence has a 97.66% homology with *Desulfosporosinus nitroreducens* and a 97.20% with *Desulfosporosinus orientis*.

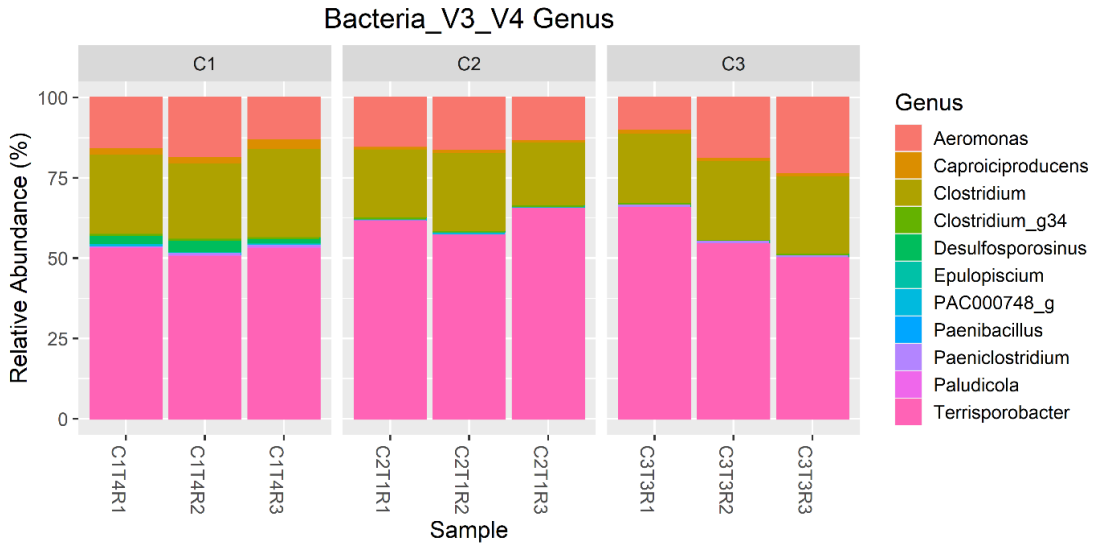

Figure 7. The microbial population analysis based on DNA-sequencing data.

The most abundant species in this consortium was probably *Terrisporobacteur petrolearius. Terrisporobacteur sp*. can grow autotrophically on H_2 and CO_2 through acetogenesis, but there is no reference for *T. petrolearius* specifically (Böer *et al.*, 2023). However, this species uses sulfite as an elector acceptor (Deng *et al.*, 2015). The second most abundant species in the samples was *Clostridium huakuii* which uses sodium sulfite as an electron donor but there is no reference of growth in the presence of H_2 and CO_2, only for closely related species (Ruan *et al.*, 2014). Moreover, the genus *Aeromonas* consists of facultative anaerobic species, like *Aeromonas hydrophila*. This species is possibly capable to reduce sulphite to H_2S, since it is mentioned bibliographically that it has been isolated by a consortium with this ability (Mcleod *et al.*, 1998). However, there is no reference of growth under H_2/CO_2 gas-phase conditions. Even if the gas-phase conditions are not the usual for *Aeromonas sp.* growth, this species is a possible participant in the studied microbial consortium. The number of the sequences is not high, so is the percentage of its presence which is verified by the speculation of the non-optimal conditions. Other than *Aeromonas hydrophila*, species with high homology are *Aeromonas enterica*, *A. bestiarum*, *A. salmonicida* and *Citrobacter freundii*.

The sequence that its presence increases from one culture to another presents a great homology with *Clostridium thailandense*, as mentioned above. This bacterium is strictly anaerobic, it has been isolated from a soil sample, and it conducts anaerobic respiration with H_2 and CO_2 (Chaikitkaew *et al.*, 2022). The profile of this microbe matches the studying consortium's one, making it a possible member of it. Furthermore, the two possible species to whom belong the sequence isolated only from the first culture, *Desulfosporosinus nitroreducens* and *D. orientis*, are bacteria able to grow anaerobically under H_2/CO_2. The first can use sulfite as an electron acceptor (Vandieken *et al.*, 2017), while the second can use sulphate, since it is characterized as a sulphate-reducing microorganism (Agostino *et al.*, 2020). In this study sulphate consumption has been observed as mentioned above. A part of the sulphate from the medium is consumed to produce the observed H_2S. Therefore, it is possible that the first species may be a part of this environmental consortium.

There are certain genera that were affiliated only in low percentages and not in all the samples as depicted in **Figure 7**. *Caproiciproducens sp* and *Paeniclostridium sp* are obligately anaerobic bacteria. The first genus has been cited to produce H_2 and CO_2 and has been isolated from a wastewater treatment plant (Jeon and Sang, 2023), while the second has been isolated from different marine sediments (Sasi Jyothsna *et al.*, 2016). *Paenibacillus sp* are facultative anaerobic bacteria and the *Paenibacillus polymyxa* species has been part of a hydrogen productive consortium (Watanapokasin *et al.*, 2009). These microorganisms could be a part of this environmental consortium because they are anaerobic ones, but this is their only characteristic that matches its profile. Finally, *Paludicola sp* is an unstudied genus that has been found in the human-gut (Wishart *et al.*, 2023), and *Epulopiscium spp* are heterotrophic bacteria that are intestinal symbionts of tropical marine surgeonfish (Miyake, Ngugi and Stingl, 2016). Thus, these genera are unlike to be a part of the environmental consortium of this study.

IV. DISCUSSION & CONCLUSIONS

The ability of a single microorganism's pure culture and an environmental microbial consortium to consume hydrogen illuminates the importance of microbial studies at an UGS. The pure culture of *Methanobacterium formicicum* presented its maximum consumption ability at 37°C, pH 7, and 0M NaCl, which is cited as the optimal growth condition (Kotelnikova, Macario and Pedersen, 1998). However, its ability to consume hydrogen and its microbial growth were significant at the higher salinity 0.5M NaCl and both at a lower (30°C) and a higher temperature (42°C). Consequently, it is not necessary the environmental conditions to be the optimum ones for one microorganism to cause H_2-reduction at a reservoir. Bibliographically methanogens' optimal temperature growth range is 15-98°C and for the pH 4.5-9 (Bhadariya *et al.*, 2024). Furthermore, the environmental microbial consortium studied as part of the ANR HyStorEn project was isolated from an aquifer where no hydrogen injection had ever occurred. Even with no injection-history a hydrogen-consuming consortium was isolated. Regarding the results of this study, its capability to consume hydrogen was great and it does not differ a lot with the pure culture's one at the non-optimal conditions.

The characterization of *Methanobacterium formicicum* 's pure culture provided data regarding the optimal conditions, the pH growth range and the mutual influence of temperature and salinity. The pH growth range was not consistent with the one mentioned in bibliography where growth and methane production have been observed at the pH range 6.5-9.2 (Kotelnikova, Macario and Pedersen, 1998). In this study the pH range for H_2-consumption and CH_4-production was 7-7.5 but no acidic pH values were tested. However, in this study the pH value was stabilized only with the addition of 3M KOH, and it was measured after the pressure in flask was fixed at 1bar of H_2/CO_2 gas. On the

contrary in the bibliography the specific pH values were reached with the use of several solvents before the addition of any gas other than nitrogen in the gas phase. The interaction between temperature and salinity has not been tested for an anaerobic microorganism before. However, at a study of four aerobic bacteria isolated from marine sources, two of whom were *Vibrio marinus* strains, the effect of salinity on the maximal growth temperature was studied (Stanley and Morita, 1968). More specifically the variation of the maximal temperature of these strains was approximately 10°C between the highest and lowest salinity tested at which growth took place. Thus, this study proves that the maximal growth temperature can be altered by changes in the salinity of the medium where the microbial growth occurs. This result verifies the observations of this study regarding the salinity and the temperature interaction since an increase at the H_2-consumption at higher salinities like 0.5M NaCl was noted when the temperature was also increased.

All these data collected from the characterization of pure cultures could be used as feedback for models designed to evaluate the compatibility of an UGSs. More specifically, a team of researchers in 2023 published a review where they described how they used already existing data from a town gas storage, and they applied them to certain models. Their goal was to simulate hydrogen reactivity by including the kinetics of the aqueous redox reactions. The microbial activity was included in two models where one was for the microbial activity after the appliance of threshold limitations and the other for the activity that follows Monod-type rate law. After the successful calibration of the bio-geochemical models they tested and by also taking into consideration the microbial activity, the evaluation of the hydrogen reactivity of certain UHS in the future can be done with a higher value of reliability (Joachim Tremosa, Rasmus Jakobsen and Yann Le Gallo, 2023). Nevertheless, a conclusion derived only based on the characterization of single-microorganism pure cultures will present certain gaps. It is highly unlikely that only one microorganism in an underground reservoir exists, and this is the reason why besides the results acquired from these models more specified for each reservoir microbial studies must follow.

A study of an environmental microbial consortium was conducted to examine the possibility of the existence of H_2-consummers at a natural site and the difference of the data that will be obtained in comparison to pure cultures. A similar study was conducted by Dohrmann and his team (Dohrmann and Krüger, 2023), who studied a formation fluid from a natural gas field representing potential UHS in porous reservoir rock. The possibility of microbial-H_2-consumption was tested, and the effect of pressure fluctuation was examined. This fluctuation was simulating the cycles of H_2-injection and withdrawal. The effect of temperature variation was also studied. After the incubation experiments a population characterization occurred for this sample with 16S rDNA Illumina sequencing. The formation fluid consumed the sulphate that was present in the culture, which was also observed with the consortium of this study. Additionally, they observed that if sulphate was added again in the culture, the H_2-consumption rate could be recured. The microbial population prior to hydrogen injection of the formation fluid was tested, too. Some genera that are possible acetogens were affiliated, *Sphaerochaeta* and *Paramaledivibacter* sp, and a sulphate reducer, *Desulfovibrio* sp. The population was also characterized after a hydrogen injection, where the microbial population was altered both in composition, because a methanogenic genus was found (*Methanolobus* sp), as in the relative abundance and the syntrophic relationships in the community. The composition of this natural formation fluid and the microbial consortium of this study present similar groups of H_2-metabolizing microorganisms.

The study of an environmental sample directly from the location of a possible UHS reservoir provides a larger quantity of data regarding the consequences of H_2 injection. The interpretation of the data will be more complicated than the ones from pure cultures since more parameters are affecting the

outcome of such an endeavor. Both microbial diversity and the environmental conditions will alter during the usage of the reservoir for hydrogen storage. However, the environmental conditions can be measured, and the microbial population can be characterized by providing better insight into the suitability of the reservoir. The characterization of the microbial population will illuminate the possible setbacks of an H_2-injection, such as H_2-consumption and the production of other gases that will alter the composition of the stored gas. The different organisms that could be a part of an environmental population like this should be well characterized. A thorough knowledge of these microorganisms is needed to predict their activity after hydrogen injection. Thus, the study of pure cultures is also of great importance.

Hydrogen is preferred to be stored in depleted oil and gas fields, saline aquifers, and salt caverns. This arises several issues, one of which is the decrease in the concentration of stored hydrogen due to microbial activity. Before using a specific reservoir as a hydrogen storage site, several studies must be conducted. This work highlights the importance of a prior microbiological study at these sites. Both liquid and solid samples must be collected for the characterization of the already existing microbial population. The solid samples are important for the better examination of the biofilm-forming microorganisms. In order for the affiliation to be executed with a greater sensitivity to reach the species level, RNA could be extracted and sequenced from the sample. The characterization of the population to the species level contributes great knowledge on the activity of these microorganisms under the conditions developed after the H_2-injection. Furthermore, the RNA-sequencing based methods provide information about the composition of the population but not for the exact proportion between its members. Real-time quantitative PCR (RT qPCR) could help to gather more data regarding the microbial consortium (Taylor *et al.*, 2010; Bhadariya *et al.*, 2024). RT qPCR is used to detect and quantify RNA in a short span of time and the quantification of the microbial load in the sample can follow. The number of microbes can be enumerated by calculating the number of copies of targeted gene sequences. After obtaining all this data a synthetic ecology study can follow. More specifically, using pure cultures of the identified microorganisms in these samples, the environmental consortium can be synthesized in vitro. The pure cultures that will be used must be characterized. This synthetic consortium will be studied, providing all the necessary data to predict the consequences derived by the microorganisms. The knowledge obtained through laboratory experimentation can provide a microbiological stimulation process that will help to understand the interaction of microorganisms with the UHS environment.

V. Task 2 & 3 Introduction and Objectives

The global transition to renewable energy has created a strong demand for efficient energy storage systems, with hydrogen emerging as a key player due to its versatility and carbon-free combustion properties (*IEA*, 2021). Underground hydrogen storage (UHS) is seen as a promising solution to store excess hydrogen produced from renewable sources, especially during periods of low demand or surplus generation. This hydrogen can then be retrieved during peak energy demand ("Gas to Power"), contributing to the stability and resilience of energy grids. Various geological formations such as salt caverns, depleted gas reservoirs, and deep aquifers are being considered for UHS due to their ability to safely contain large volumes of gas at high pressures (Heinemann *et al.*, 2021). UHS has the potential to enable the hydrogen economy by providing large-scale, long-term energy storage, a critical element for achieving global carbon neutrality targets.

Types of Underground Hydrogen Storage (UHS)

Salt caverns are among the most widely studied geological structures for UHS due to their impermeability and ability to endure multiple storage cycles without significant degradation (Lord *et al.*, 2014). These caverns have been used successfully for natural gas storage, making them a viable option for hydrogen. Depleted gas reservoirs also offer large storage capacities and have the advantage of existing infrastructure that can be repurposed, although the potential for hydrogen diffusion through reservoir rock must be carefully assessed. Aquifers, another potential option, present challenges related to the stability of hydrogen–water interfaces and microbial activity that may result in hydrogen consumption (Heinemann *et al.*, 2021). Additionally, there is a significant lack of data regarding the reservoir formations, caprocks, and fluids, resulting in high uncertainty during the development and operation phases (Beckman *et al.*, 1995). For effective gas storage in aquifers, the reservoir rocks must exhibit favourable petrophysical properties, and the caprock must demonstrate excellent tightness and integrity to prevent any gas leakage (Tarkowski, 2019). The selection of appropriate storage sites depends on detailed geological and geochemical analyses to ensure the safety, efficiency, and longevity of UHS systems.

Challenges and risks of UHS

While UHS offers numerous advantages, it is not without challenges. The injected hydrogen interacts with the subsurface environment in multiple ways, including physical, geochemical, and microbial interactions. Physically, hydrogen diffusion and migration within porous media can lead to uneven distribution, while changes in reservoir pressure and temperature during injection and withdrawal cycles can affect storage integrity. Geochemically, hydrogen can react with minerals, leading to alterations in reservoir rock properties, including dissolution and precipitation of minerals that affect porosity and permeability. Microbial interactions are particularly significant, as microbial communities naturally present in subsurface environments can consume hydrogen as an energy source, leading to the production of secondary gases, such as hydrogen sulfide (H2S) and methane (CH4). Among these challenges, microbial interactions can directly impact storage efficiency, gas purity, and reservoir integrity. The subsurface environment hosts diverse microbial communities, including hydrogenotrophic methanogens, sulfate-reducing microorganisms (SRMs), acetogens, and iron-reducing bacteria. These microbes utilize hydrogen as an electron donor for metabolic processes, leading to several

biogeochemical reactions. Hydrogenotrophic methanogens convert hydrogen and carbon dioxide into methane, while SRMs reduce sulfate to hydrogen sulfide. Acetogens produce acetate from hydrogen and carbon dioxide.

Modelling Approaches for UHS

Given the complexity and potential risks associated with microbial activity in underground hydrogen storage, predictive modelling plays a crucial role in understanding and managing these interactions. Numerical models allow for the simulation of biogeochemical processes under varying reservoir conditions, enabling stakeholders to predict hydrogen loss by quantifying hydrogen consumption rates under different conditions. These models can estimate the extent of hydrogen loss during storage periods and assess gas purity by predicting the production of secondary gases like H_2S and CH_4, ensuring the quality of the recovered hydrogen.

Modelling also helps evaluate reservoir integrity by predicting changes in porosity, permeability, and reservoir pressure due to microbial-induced mineralization and biofilm formation. It optimizes storage operations by simulating different injection and withdrawal scenarios, informing operational strategies to minimize hydrogen loss and mitigate microbial risks. Moreover, it guides site selection by understanding the site-specific microbial community and its metabolic potential, helping to select suitable storage sites with minimal microbial activity. For the goals of Task 2 of deliverable 4.2, we tested two such models that are described below.

VI. Task 2-The DuMux Model

One of the most advanced modeling frameworks for UHS is DuMu^x, an open-source simulation tool for multi-phase flow and transport in porous media (Flemisch *et al.*, 2011). DuMu^x is particularly well-suited for UHS applications because it can simulate complex interactions such as gas migration, diffusion, and dissolution, as well as thermal effects and geochemical responses. By incorporating realistic boundary conditions and coupling multi-physics processes, DuMu^x enables researchers to predict hydrogen behavior under various geological and operational scenarios (Flemisch *et al.*, 2011). This capability is crucial for optimizing storage strategies and mitigating risks such as leakage or unintended hydrogen migration, which could compromise storage integrity or lead to environmental impacts. DuMu^x has become a critical tool for the development of safe, efficient, and economically viable UHS solutions.

Here, we simulating underground town gas storage using real data from the Lobodice aquifer in the Czech Republic, following the work of Ahmadpour, 2022 and based on field data provided by the study of Hogeweg, *et al.* 2022. The simulations utilized available data, including the molar composition of the injected and produced gases after seven months of storage, with an emphasis on understanding the role of methanogenic activity. The primary objective was to match the gas production data generated by DuMu^x software to actual field data by tuning specific parameters, such as injection rates and the growth and yield rates of studied methanogens. A simplified geological model was employed for history matching, and parameter adjustments were used to replicate observed gas composition changes. For future studies, incorporating microbial growth, decay rates, and substrate consumption data for methanogens, sulfate-reducing bacteria (SRBs), and acetogens could improve the accuracy of

these simulations and enhance understanding of subsurface microbial processes during UGS operations.

VII. Experimental Design and Methodology

Study site

The Lobodice aquifer, located in the Czech Republic, is a constructed aquifer which serves as an underground gas storage (UGS) facility. The geological structure of the aquifer consists of basal clastics, with an average porosity of 24%, allowing for significant storage capacity for gas. This aquifer lies at depths of approximately 400–500 meters and is underlain by a layer of Neocene Baden sediments, which are predominantly calcareous clays (Kopal, *et al.* 2016). These sediments, with their substantial thickness, act as an effective seal, preventing gas migration beyond the designated storage area. The aquifer's initial saturation with seawater, combined with the natural compaction and diagenesis processes, contributes to its ability to store fluid, making it suitable for gas injection and withdrawal. The hydrogeological properties of the aquifer, including its permeability and porosity, were assessed revealing a complex but stable storage structure that accommodates gas injection with minimal risks of leakage (Tremosa *et al.*, 2023, Kopal, *et al.* 2016).

After several months of active gas storage, detailed monitoring and analysis were conducted to assess the integrity of the Lobodice aquifer under operational conditions. Observations showed that the reservoir's pressure distribution remained consistent, with no significant anomalies indicative of gas migration outside the designated storage zone (Kopal, *et al.* 2016). Seismic surveys confirmed the absence of substantial fractures or faults that could compromise the seal provided by the Neocene Baden layer. However, some variations in pressure gradients were observed, suggesting localized heterogeneity within the aquifer that may affect the efficiency of gas distribution during injection and withdrawal cycles. These findings underscore the importance of continuous monitoring, as they highlight the necessity of optimizing injection strategies to accommodate the natural heterogeneity of the aquifer. Furthermore, the data collected has been pivotal in refining models that predict the long-term behavior of the aquifer under sustained gas storage operations, ensuring both the operational safety and economic viability of the facility for future use.

The Lobodice aquifer has a storage capacity of 100 million cubic meters and a daily production capacity of 1 million cubic meters of coal gas (commenced by first injection on May 25, 1965). Extension of technology and additional withdrawal and injection wells were completed in 1975. In 1990, when last coal gas was withdrawn, the underground gas storage was switched over to the natural gas (https://www.czgs.cz/en/about-us/our-storages/lobodice). Data from town gas storage after a 7-month period indicated a loss in H_2 and an increase in CH_4, which could potentially be the work of methanogenic microorganisms.

Model description

DuMu^x (Version 3.7) is written in C++ and is based on the DUNE framework. It uses DUNE's versatile grid interface, vector and matrix types, geometry and local basis functions, and linear solvers. It can provide:

- Finite volume discretizations and control-volume finite element discretization schemes.

- A flexible system matrix assembler and approximation of the Jacobian matrix by numeric differentiation.
- A customizable Newton method implementation including line search and various stopping criteria.
- Many pre-implemented models (Darcy-scale porous media flow, Navier-Stokes, Geomechanics, Pore network models, Shallow water equations) and constitutive models.
- A multi-domain framework for model coupling suited to couple subproblems with different discretizations/domains/physics/dimensions/etc and create monolithic solvers (https://dumux.org/docs/doxygen/master/index.html).

DuMu^x, in its current version (3.7), has integrated biochemical reactions involving methanogens and sulphate-reducing bacteria (SRBs), though SRBs remain inactive at present. This integration allows users to adjust key microbial parameters, such as growth rates, decay rates, and yield, offering a significant advantage over commonly used commercial simulators like Eclipse. While DuMu^x is still in its developmental stages, the inclusion of biochemical reactions is vital for accurately modelling Underground Gas Storage (UGS) systems, as microbial processes can influence gas composition and reservoir dynamics. DuMu^x models microbial dynamics by coupling mass balance equations with microbial population models, represented by a set of differential equations that describe growth and decay processes. By incorporating these dynamics into the larger reservoir model, DuMu^x simulates the potential effects of microbial activity, particularly focusing on the production of hydrogen sulfide (H_2S) in UGS environments. In this study, the microbial growth rate and yield values used for methanogens were based on data from Thaysen *et al.* (2021), which provides insights into microbial growth and hydrogen consumption in porous media.

DuMu^x runs in Linux operating system, hence when working from Windows, Windows Subsystem for Linux (WSL) and Ubuntu are essential to run the code.

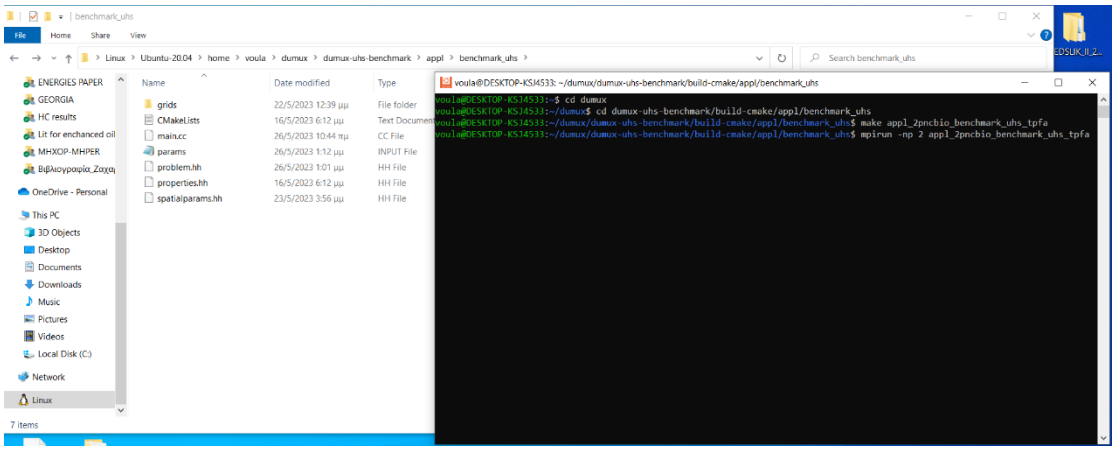

Figure 1. On the left, the directory where the main code is located. On the right, the Ubuntu window where the functions are called.

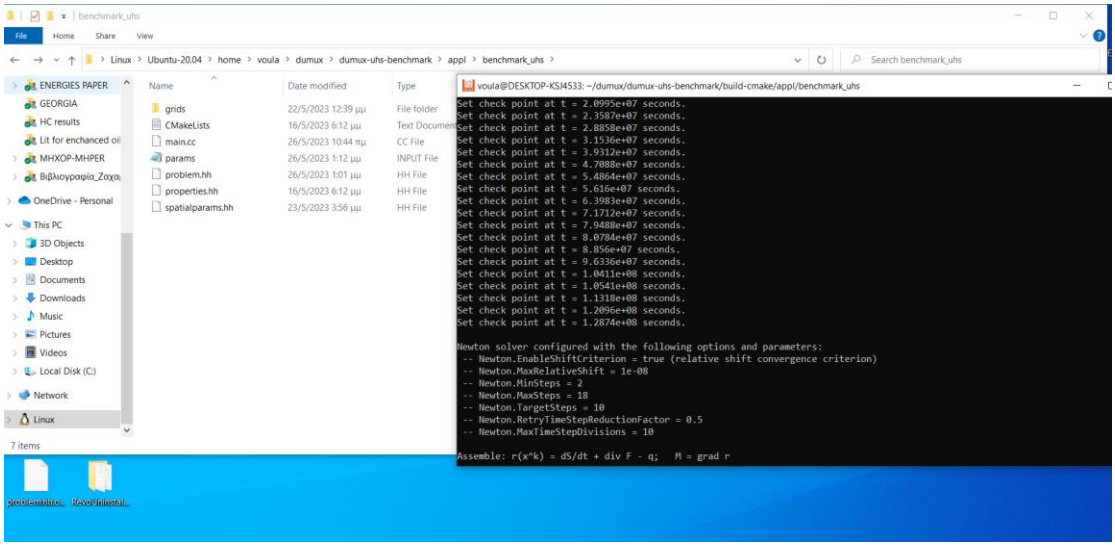

Figure 2. On the left, the directory where the main code is located. On the right, the Ubuntu window while the code is running.

Numerical Simulations: UGS simulation and biochemical reactions

The current version of DuMu^x (3.7) incorporates several key features for simulating underground gas storage (UGS) and biochemical reactions. These include the ability to specify the growth rate, decay rate, and yield for methanogens, as well as parameters for homogeneity, permeability, and porosity, which are essential for modelling the reservoir. Other critical factors include the injection and production rates, depth of injection, well position, and reservoir grid, which can be generated in PETREL software and exported as a .GRDECL file. Additionally, the simulation allows for temperature, pressure, water, and gas saturation, as well as molar composition of injected gases, with a simulation time adjustable to fit the desired modelling period.

For the UGS simulation in this study, a homogeneous corner point reservoir with 22x32x5 grid cells (Ahmadpour, 2022) was integrated in the code to replace the much larger heterogeneous reservoir from the case study of Hogeweg *et al.* (2022), with one well for injection and production, located at the centre of the reservoir.

Typical values of water density and pressure at Gas-Water Contact (GWC) in an aquifer, based on temperature and height, were used in the software. The GWC was set at a depth of 1,050 m and pressure at 5 MPa.

Due to the lack of data regarding the reservoir (only known value was the porosity 0.24), permeability values were chosen accordingly to avoid fracturing of the formation due to the pressure rise during the injection process (~500 mD).

Scalar density of water (brine) was set at 1,020 kg/m^3 and scalar density of gas was estimated at 86 kg/m^3.

The molar composition of gases according to data from the Lobodice was:

Table 1. Molar composition of gases at the injection and production from the Lobodice aquifer.

Component gas	Molar composition of gases at Injection	Molar composition of gases at Production, after 7 months of storage
H_2	54%	37%
N_2	2.5%	8.6%
CO_2	11.67%	8.78%
CO	9%	3.3%
CH_4	21.9%	40%
C_2H_4+C_2H_6	0.41%	0.53%
C_3+	0.09%	0.18%

Cell numbers of methanogens in the formation water of the Lobodice aquifer were 10^3-10^4 cells/mL.

Initial temperature of the reservoir was assumed to be at 37 ^oC, an optimal temperature for the growth of certain methanogenic species.

Connate water saturation was assumed: S_{wr} = 0.2 and residual gas saturation: S_{nr} = 0.05.

Running time was set at 7 months, with a timestep of 1,000 s and starting point at 1,000 s.

To the best of our knowledge, this version of DuMu^x doesn't involve any data for pH values or salinity.

Visualization of the results

When running is complete, DuMu^x creates files with the results in a subfolder. These files include well rates over time, converted gases rates from microbial activity, bottom hole pressure over time and more. The data produced, can be further analysed in Excel or with other data analysis tools. The visualization of the results is possible using Paraview, an open-source platform that allows you to perform data analysis and visualization (Henderson, 2007).

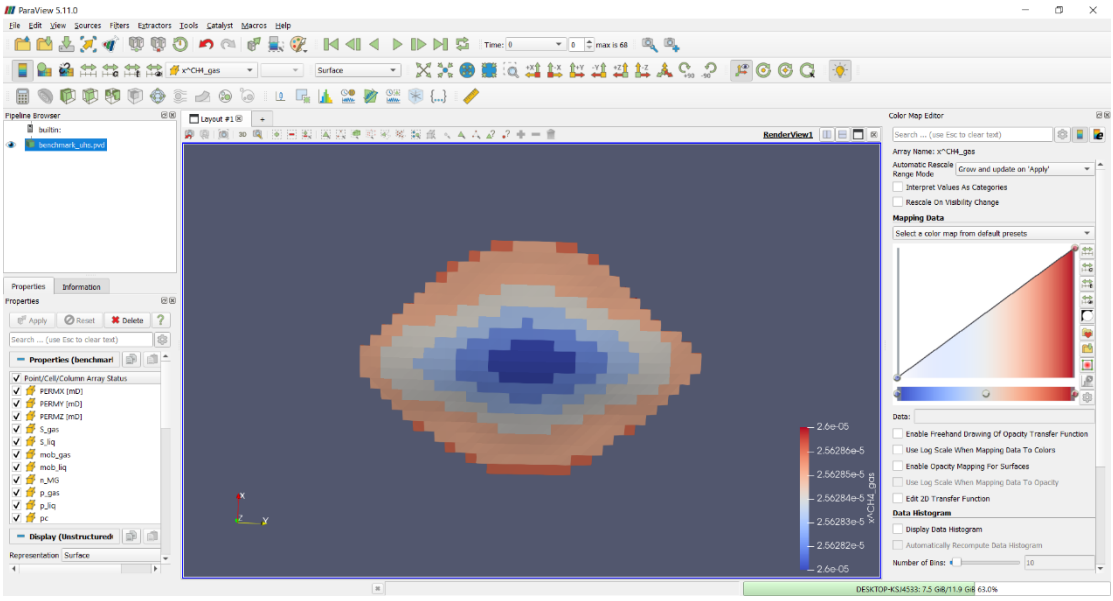

Figure 3: Paraview interface. In the upper left corner, the file containing the produced results is imported; in the lower left, various properties can be selected to apply to the reservoir model; in the centre, the 3D reservoir model displays changes in properties over time; and on the right, the data analysis panel allows users to select properties and generate graphs to visualize the changes over time.

VIII. Results

The optimized values of the tuning parameters (injection rate, maximum growth rate and yield) were:

Injection rate (gmole/s): 3000,

Maximum Growth rate of methanogens (1/s): $1.6 \cdot 10^{-5}$,

Yield (g/gmole of H_2): $5 \cdot 10^{8}$.

The final molar composition of gases after the tuning is presented in Table 2.

Table 2. Molar composition of gases at the production of the Lobodice aquifer from field data and production according to DuMu^x simulations after tuning biochemical parameters.

Component gas	Molar composition of gases at Production_Field Data	Molar composition of gases at Production_Simulations
H_2	37%	37.61%
N_2	8.6%	12.09%
CO_2	8.78%	8.91%
CO	3.3%	0.02%
CH_4	40%	40.65%
C_2H_4+C_2H_6	0.53%	0.54%
C_3+	0.18%	0.18%

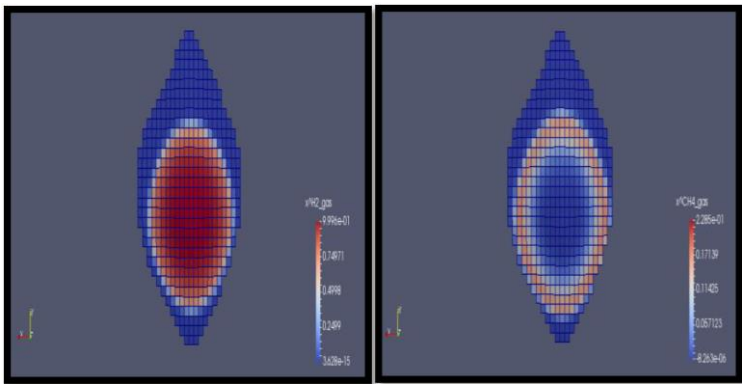

Figure 4: Final H_2 concentration distribution on the left and CH_4 concentration distribution on the right.

Simulations indicated that utilizing a single well for both injection and production requires careful management of operational parameters to achieve optimal results. A low injection rate was found to be insufficient for meeting operational demands. With reduced injection rates, gravitational segregation of gases becomes more pronounced, leading to greater separation and inefficiencies. Additionally, maintaining adequate reservoir pressure for the withdrawal process necessitates a controlled production rate to avoid rapid pressure declines.

Increasing the injection rate should be approached with caution to prevent fracturing of the formation, especially when using a single well where injection and production cycles are interdependent.

1.2 Concluding remarks

The simulations conducted in this study demonstrated that by adjusting the growth rate and yield of certain methanogenic microorganisms, a close approximation to the observed field data could be achieved. The injection rate was also found to be a critical factor influencing bio-methanation in the modelling scenarios. The lack of extensive documentation on underground microbial activity and the limited data available on the reservoir properties prevent us from conclusively attributing the observed decrease in hydrogen (H_2) during town gas storage to microbial processes. Additionally, the accuracy of the applied values for the methanogen growth rate and yield remains uncertain, as these parameters have not been validated through additional experimentation with subsurface microbial communities. This uncertainty underscores the need for further investigations to confirm the role of microbial activity in gas composition changes within underground gas storage (UGS) facilities. Moreover, the exclusion of sulfate-reducing bacteria (SRBs) and acetogenic bacteria, which are known to influence biochemical processes in subsurface environments, further limits the comprehensiveness of the model. Their biochemical reactions were not incorporated into this study due to current limitations in the Dumux software, which does not yet integrate these processes in its latest version.

To improve the understanding of UGS systems and their associated biochemical reactions, additional data on microbial activity in the subsurface and a more thorough characterization of the reservoir's properties are essential. While Dumux proves to be a valuable tool for simulating biogeochemical processes in UGS systems, particularly in its capacity to adjust correlations and

implement biochemical reactions more effectively than commercial simulators like Schlumberger's ECLIPSE, it still requires further refinement. With enhanced integration of microbial data and more accurate representation of subsurface microbial processes, Dumux could significantly improve the prediction of UGS performance and future trends. These advancements would not only optimize gas storage operations but also contribute to more sustainable and efficient management of UGS facilities, ensuring their viability in the long term.

IX. Task3 - Custom Python-based model

Methodology

Microbial Data Collection

The foundation of this study was built upon comprehensive data collection from peer-reviewed scientific literature, technical reports, and reputable databases. The primary focus was to gather parameters relevant to microbial activity in underground hydrogen storage environments. These parameters included microbial growth rates, substrate affinities, product yields, and environmental conditions such as temperature, pressure, salinity, and pH that influence microbial metabolism. To ensure the accuracy and relevance of the collected data, a systematic literature review was conducted, and studies were screened based on relevancy. Priority was given to studies published within the last ten years, reporting field and quantitative data on microbial reactions under conditions mimicking underground storage environments. From the selected studies, key parameters were extracted, including:

- Microbial Kinetics: Maximum specific growth rates (μmax), half-saturation constants (Ks), and inhibition constants.
- Reaction Stoichiometry: Consumption of hydrogen and production of methane, hydrogen sulphide, and acetate.
- Environmental Conditions: Temperature, salinity, pH, and pressure ranges that affect microbial activity.
- Mineral Reactions: Dissolution and precipitation rates associated with microbial by-products.

Cross-Verification: The extracted data were cross-referenced with multiple sources to validate accuracy and consistency. In cases where discrepancies were identified, the most conservative values were adopted to ensure the robustness of the simulations. The final dataset served as the input for the numerical modelling, enabling the simulation of microbial interactions in underground hydrogen storage environments.

Simulation Approach

To simulate the microbial processes and their geochemical impacts, a multi-faceted numerical modelling approach was employed. The simulation framework integrated microbial kinetics, geochemical reactions, and transport processes to capture the dynamic behaviour of underground hydrogen storage systems. The model was developed based on a system of ordinary differential equations (ODEs) representing the biogeochemical reactions. These equations accounted for hydrogen consumption, microbial growth, product formation

(methane, hydrogen sulphide, acetate), and associated mineral reactions. The growth of sulphate-reducing microorganisms (SRMs), methanogens, and acetogens was modelled using Monod kinetics, expressed as:

$$dB/dt=\mu\_max\times S/(K+S)\times B-d\times B$$

where B represents microbial biomass concentration, μmax is the maximum specific growth rate, S is the substrate concentration (H2 or sulphate), K is the half-saturation constant, and d is the decay rate.

Key geochemical reactions including methanogenesis and sulphate reduction were then incorporated together with mineral precipitation and dissolution reactions, such as the formation of calcium carbonate (CaCO3) and iron sulphide (FeS). The simulation was performed under conditions representative of underground storage sites: temperature range of 30-80°C, salinity of 0-1.5 M NaCl, and pressure of 10-50 MPa. The initial pH was set at 7.0, with dynamic changes driven by microbial activity. The system of ODEs was solved using the Python library SciPy, specifically the odeint solver. A time span of 365 days was simulated, with results recorded at daily intervals.

Model Development

The model was developed using Python, with key libraries including NumPy for numerical operations, SciPy for solving ordinary differential equations (ODEs), and Matplotlib for visualization. The core of the model comprised a system of ODEs representing microbial growth, substrate consumption, product formation, and geochemical transformations.

The microbial kinetics were modelled using Monod-type equations, where the growth rate depended on hydrogen availability and environmental conditions. Each microbial group—hydrogenotrophic methanogens, sulphate-reducing microorganisms (SRMs), acetogens, and iron-reducing bacteria—was represented as a distinct population with specific kinetic parameters derived from literature.

Parameterization

Model parameters were defined based on the comprehensive database compiled during the literature review. These parameters included maximum specific growth rates, substrate affinities, yield coefficients, and decay rates for each microbial group. Environmental parameters, such as temperature, pH, and salinity, were also incorporated to reflect realistic reservoir conditions. Key parameters included:

- Maximum specific growth rate (μmax): The highest rate at which microbial populations can grow under optimal conditions.
- Half-saturation constant (Ks): The substrate concentration at which microbial growth reaches half its maximum rate.
- Yield coefficient (Y): The amount of microbial biomass produced per unit of substrate consumed.
- Decay rate (d): The rate at which microbial biomass decays over time.

Model Execution

The model was executed using the SciPy odeint function, which numerically solved the system of ODEs over a defined simulation period. Initial conditions were set based on typical reservoir conditions, including hydrogen partial pressure, microbial biomass concentrations, and background geochemistry. Simulation outputs included time-series data for hydrogen concentration, microbial biomass, secondary gas production (H2S and CH4), pH, and mineral precipitation. These outputs were visualized using Matplotlib, facilitating the interpretation of microbial dynamics and their impact on reservoir conditions.

Validation and Sensitivity Analysis

To ensure model accuracy, simulation results were compared with experimental data from published studies. Sensitivity analyses were performed to evaluate the influence of key parameters on model outputs, identifying critical factors affecting hydrogen consumption and byproduct generation. Overall, the Python model implementation provided a robust framework for understanding the complex interplay between microbial activity and geochemical processes in underground hydrogen storage environments, guiding the development of effective management strategies.

X. Results and Discussion

Hydrogen Consumption Dynamics

The simulation results revealed a significant consumption of hydrogen due to microbial activity (see Figure 1). The consumption was primarily driven by hydrogenotrophic methanogens and sulphate-reducing microorganisms (SRMs), with the rate of consumption varying based on environmental conditions, hydrogen availability, and microbial growth dynamics. Hydrogen consumption followed a biphasic pattern. In the initial phase, rapid hydrogen consumption occurred as microbial populations grew exponentially. This phase corresponded to the peak microbial metabolic activity. The second phase exhibited a slower consumption rate as hydrogen availability decreased, leading to substrate limitation.

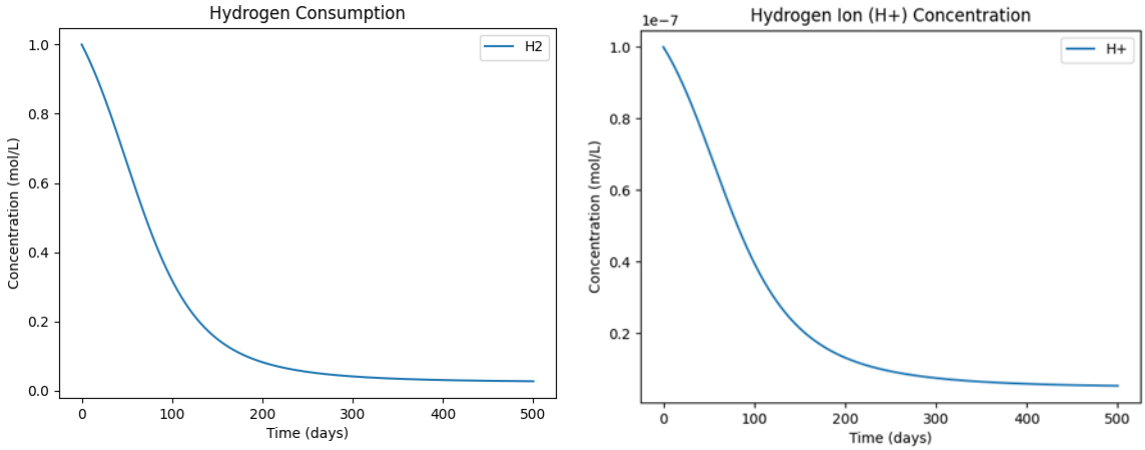

Figure 1: Hydrogen consumption due to the microbial activity

The simulation confirmed that hydrogenotrophic methanogenesis was dominant under sulphate-limited conditions. In contrast, under sulphate-rich conditions, SRMs outcompeted methanogens, consuming hydrogen to reduce sulphate and produce hydrogen sulphide. The competition between methanogens and SRMs was influenced by pH, temperature, and salinity. Higher temperatures favoured methanogenesis, while increased salinity inhibited both microbial groups. Sensitivity analysis demonstrated that hydrogen consumption was most sensitive to microbial growth rates and hydrogen availability.

Production of Secondary Gases: H2S and CH4

The simulation showed that hydrogen consumption led to the production of secondary gases, including hydrogen sulphide (H2S) and methane (CH4), depending on the prevailing microbial pathway (see Figure 2). Under sulphate-rich conditions, H2S production dominated, while methane production was prominent when sulphate was depleted. These findings highlight the importance of monitoring secondary gas production to maintain gas purity and reservoir integrity.

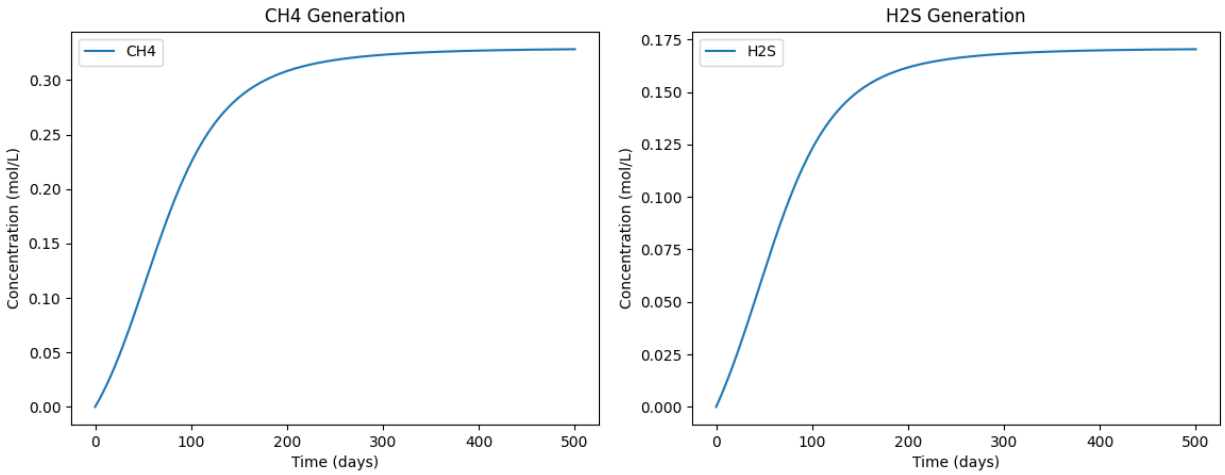

Figure 2: CH4 and H2S generation due to the microbial activity

Microbial Biomass Growth

Microbial biomass growth was closely linked to hydrogen availability and environmental conditions. The simulation showed distinct growth patterns for SRMs and methanogens (see Figure 3). Biomass accumulation was rapid during the initial phase of hydrogen injection and sulphate availability. As sulphate was depleted, SRM growth slowed, with biomass decay driven by endogenous respiration. Methanogens exhibited slower growth compared to SRMs but continued accumulating biomass as long as hydrogen and carbon dioxide were available. The yield coefficient for methanogens was consistent with literature values, validating the model's accuracy. Microbial decay contributed to organic byproduct formation, further altering reservoir conditions and influencing hydrogen transport.

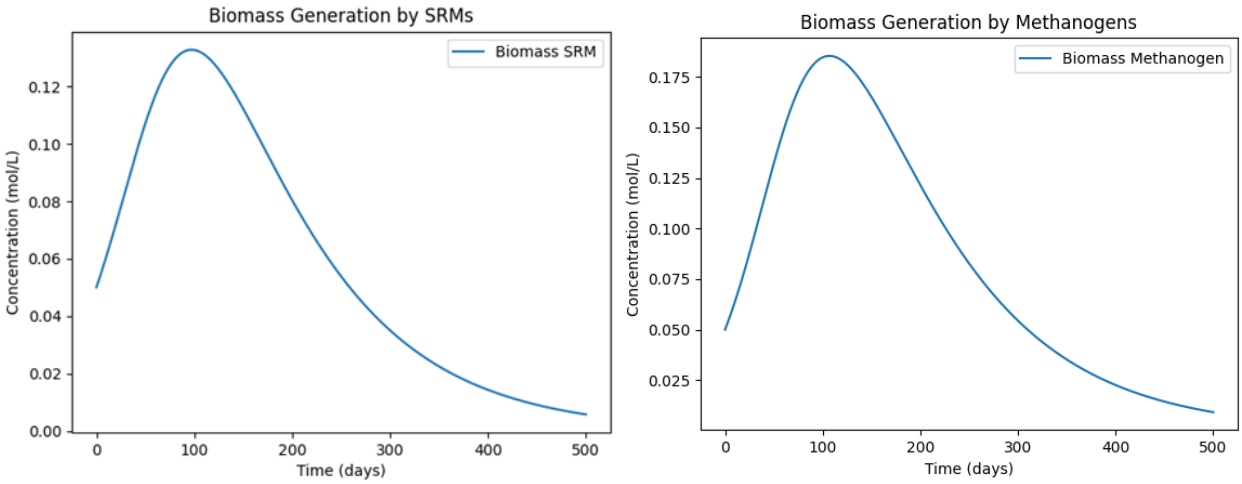

Figure 3: Microbial biomass growth for SRMs and methanogenesis

The simulation also tracked biomass growth and pH changes over time. Microbial populations expanded rapidly during the initial hydrogen injection phase, with SRMs dominating in sulphate-rich conditions and methanogens thriving as sulphate was depleted. It appeared that:

- SRMs exhibited rapid growth, peaking during hydrogen and sulfate availability.
- Methanogen biomass increased gradually, persisting longer due to sustained hydrogen consumption.
- Initial pH increases during methanogenesis, promoting carbonate precipitation.
- Localized pH reduction near SRM activity due to H2S production.
- Stabilization of pH as microbial activity declined, and mineral buffering occurred.

<u>pH Evolution and Geochemical Changes</u>

The simulation revealed significant pH changes driven by microbial activity and associated geochemical reactions (see Figure 4). The trends varied depending on the dominant microbial pathway:

- **Methanogenesis:** Increased pH due to hydroxide ion release during hydrogen consumption. This alkalinization promoted calcium carbonate precipitation, potentially clogging pore spaces.

- **Sulphate reduction:** Localized acidification occurred due to H2S production, enhancing mineral dissolution and iron sulphide formation.
- **Acetogenesis:** Acetate production led to slight pH reduction, promoting mineral dissolution and carbonate equilibrium shifts.

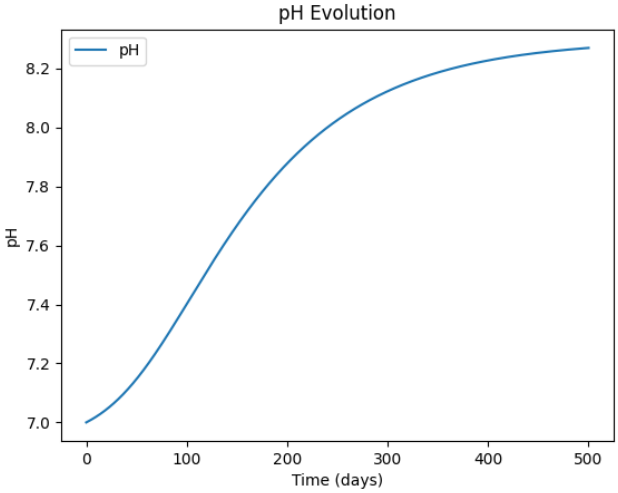

Figure 4: Changes in pH due to the microbial activities

Mineral Precipitation and Porosity Reduction

Microbial activity and associated geochemical changes led to significant mineral precipitation, reducing reservoir porosity and permeability. Key precipitation reactions included: **Calcium Carbonate (CaCO3) Precipitation** and **Iron Sulphide (FeS) Formation** -facilitated by H2S production during sulphate reduction- and **Silica Dissolution -** enhanced under localized acidic conditions, further altering rock matrix integrity. This precipitation can cause porosity reduction near hydrogen injection points, where microbial activity and geochemical transformations are concentrated. Biofilm formation can also cause exacerbated pore clogging, reducing injectivity and permeability.

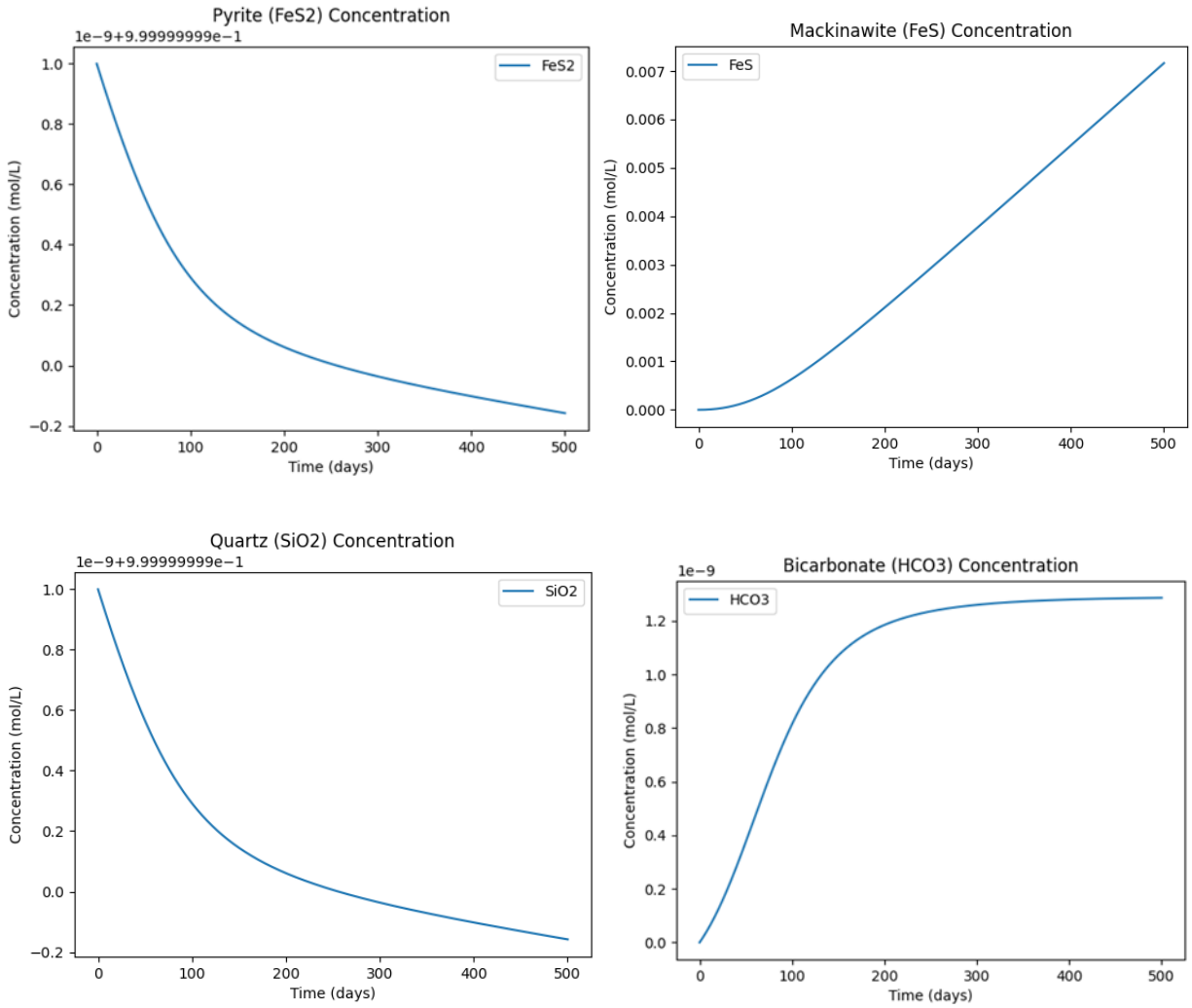

Figure 5: Mineral precipitation due to the microbial activity and geochemical reactions

Implications for Underground Hydrogen Storage

The simulation findings have significant implications for the design, operation, and management of underground hydrogen storage systems:

1. **Hydrogen Loss:** Microbial consumption can lead to substantial hydrogen loss, reducing storage efficiency.
2. **Gas Purity:** H2S and CH4 production compromises gas purity, necessitating monitoring and treatment.
3. **Reservoir Integrity:** Mineral precipitation and biofilm formation reduce porosity and permeability, affecting injectivity and withdrawal rates.
4. **Operational Optimization:** Understanding microbial dynamics enables optimization of injection and withdrawal cycles, minimizing hydrogen loss.

XI. Conclusion and Future Work

The simulation results demonstrate that microbial activity significantly influences underground hydrogen storage, affecting hydrogen availability, gas purity, and reservoir integrity. The findings underscore the need for site-specific microbial assessments, continuous monitoring, and adaptive management practices to mitigate microbial risks and optimize storage performance. This comprehensive understanding provides a foundation for future research, guiding the development of resilient and sustainable underground hydrogen storage systems.

While the simulation provided valuable insights, certain limitations should be acknowledged:

- **Simplified Microbial Community**: The model focused on dominant microbial groups (SRMs, methanogens, acetogens, IRBs), excluding less abundant species that may influence reservoir dynamics.
- **Site-Specific Variability**: Model parameters were based on generalized conditions, potentially underrepresenting site-specific variations.
- **Long-Term Dynamics**: The simulation covered a limited time frame; further studies are needed to assess long-term microbial and geochemical evolution.

Future work should focus on integrating field data from hydrogen storage sites, expanding microbial community models, and simulating long-term storage scenarios under varying operational conditions.

XII. REFERENCES

Agostino, V. *et al.* (2020) 'Electrophysiology of the Facultative Autotrophic Bacterium Desulfosporosinus orientis', *Frontiers in Bioengineering and Biotechnology*, 8, p. 538436. Available at: https://doi.org/10.3389/FBIOE.2020.00457/BIBTEX.

Bartoš, O., Chmel, M. and Swierczková, I. (2024) 'The overlooked evolutionary dynamics of 16S rRNA revises its role as the "gold standard" for bacterial species identification', *Scientific Reports 2024 14:1*, 14(1), pp. 1–9. Available at: https://doi.org/10.1038/s41598-024-59667-3.

Bhadariya, V. *et al.* (2024) 'Hydrogen storage in porous media: Understanding and mitigating microbial risks for a sustainable future', *International Journal of Hydrogen Energy*, 67, pp. 681–693. Available at: https://doi.org/10.1016/J.IJHYDENE.2024.04.178.

Böer, T. *et al.* (2023) 'Genome-based metabolic and phylogenomic analysis of three Terrisporobacter species', *PLOS ONE*, 18(10), p. e0290128. Available at: https://doi.org/10.1371/JOURNAL.PONE.0290128.

bp (2023) 'British Petroleum. Energy Outlook'. Available at: https://www.bp.com/en/global/corporate/energy-economics/energy-outlook.html (Accessed: 18 February 2024).

Chaikitkaew, S. *et al.* (2022) 'Clostridium thailandense sp. nov., a novel CO2-reducing acetogenic bacterium isolated from peatland soil', *International Journal of Systematic and Evolutionary Microbiology*, 72(2), p. 005254. Available at: https://doi.org/10.1099/IJSEM.0.005254/CITE/REFWORKS.

Deng, Y. *et al.* (2015) 'Terrisporobacter petrolearius sp. Nov., isolated from an oilfield petroleum reservoir', *International Journal of Systematic and Evolutionary Microbiology*, 65(10), pp. 3522–3526. Available at: https://doi.org/10.1099/IJSEM.0.000450/CITE/REFWORKS.

Dohrmann, A.B. and Krüger, M. (2023) 'Microbial H2 Consumption by a Formation Fluid from a Natural Gas Field at High-Pressure Conditions Relevant for Underground H2 Storage', *Environmental Science and Technology*, 57(2), pp. 1092–1102. Available at: https://doi.org/10.1021/ACS.EST.2C07303/SUPPL_FILE/ES2C07303_SI_001.PDF.Dopffel, N. *et al.* (2023) 'Microbial hydrogen consumption leads to a significant pH increase under high-saline-conditions– implications for hydrogen storage in salt caverns'. Available at: https://doi.org/10.21203/RS.3.RS-2854152/V1.

Dopffel, N., Jansen, S. and Gerritse, J. (2021) 'Microbial side effects of underground hydrogen storage – Knowledge gaps, risks and opportunities for successful implementation', *International Journal of Hydrogen Energy*, 46(12), pp. 8594–8606. Available at: https://doi.org/10.1016/J.IJHYDENE.2020.12.058.

Escudié, F. *et al.* (2018) 'FROGS: Find, Rapidly, OTUs with Galaxy Solution', *Bioinformatics*, 34(8), pp. 1287–1294. Available at: https://doi.org/10.1093/BIOINFORMATICS/BTX791.

Haddad, P.G. *et al.* (2022) 'Geological storage of hydrogen in deep aquifers – an experimental multidisciplinary study', *Energy & Environmental Science*, 15(8), pp. 3400–3415. Available at: https://doi.org/10.1039/D2EE00765G.

Heinemann, N. *et al.* (2021) 'Enabling large-scale hydrogen storage in porous media – the scientific challenges', *Energy & Environmental Science*, 14(2), pp. 853–864. Available at: https://doi.org/10.1039/D0EE03536J.

Jeon, B.S. and Sang, B.-I. (2023) 'Caproiciproducens', *Bergey's Manual of Systematics of Archaea and Bacteria*, pp. 1–8. Available at: https://doi.org/10.1002/9781118960608.GBM01731.

Joachim Tremosa, Rasmus Jakobsen and Yann Le Gallo (2023) 'Assessing and modeling hydrogen reactivity in underground hydrogen storage: A review and models simulating the Lobodice town gas storage', *Frontiers in Energy Research*, pp. 1–16.

Kotelnikova, S., Macario, A.J.L. and Pedersen, K. (1998) 'Methanobacterium formicicum sp. nov., a new alkaliphilic, eurythermic and halotolerant methanogen isolated from deep granitic groundwater', *International Journal of Systematic Bacteriology*, 48(2), pp. 357–367. Available at: https://doi.org/10.1099/00207713-48-2-357/CITE/REFWORKS.

Liu, N. *et al.* (2023) 'Pore-scale study of microbial hydrogen consumption and wettability alteration during underground hydrogen storage', *Frontiers in Energy Research*, 11, p. 1124621. Available at: https://doi.org/10.3389/FENRG.2023.1124621/BIBTEX.

Magoč, T. and Salzberg, S.L. (2011) 'FLASH: fast length adjustment of short reads to improve genome assemblies', *Bioinformatics*, 27(21), pp. 2957–2963. Available at: https://doi.org/10.1093/BIOINFORMATICS/BTR507.

Martin, M. (2011) 'Cutadapt removes adapter sequences from high-throughput sequencing reads', *EMBnet.journal*, 17(1), pp. 10–12. Available at: https://doi.org/10.14806/EJ.17.1.200.

Mcleod, E.S. *et al.* (1998) 'Isolation and Identification of Sulphite- and Iron Reducing, Hydrogenase Positive Facultative Anaerobes from Cooling Water Systems', *Systematic and Applied Microbiology*, 21(2), pp. 297–305. Available at: https://doi.org/10.1016/S0723-2020(98)80037-4.

Miyake, S., Ngugi, D.K. and Stingl, U. (2016) 'Phylogenetic diversity, distribution, and cophylogeny of giant bacteria (Epulopiscium) with their surgeonfish hosts in the Red Sea', *Frontiers in Microbiology*, 7(MAR), p. 171728. Available at: https://doi.org/10.3389/FMICB.2016.00285/BIBTEX.

Molíková, A. *et al.* (2022) 'Underground gas storage as a promising natural methane bioreactor and reservoir?', *Journal of Energy Storage*, 47, p. 103631. Available at: https://doi.org/10.1016/J.EST.2021.103631.

Nazina, T.N. *et al.* (2023) 'Biodiversity and Potential Activity of Microorganisms in Underground Gas Storage Horizons', *Sustainability (Switzerland)*, 15(13), p. 9945. Available at: https://doi.org/10.3390/SU15139945/S1.

Ranchou-Peyruse, M. *et al.* (2019) ‘Geological gas-storage shapes deep life’, *Environmental Microbiology*, 21(10), pp. 3953–3964. Available at: https://doi.org/10.1111/1462-2920.14745.

Ruan, Z. *et al.* (2014) ‘Clostridium huakuii sp. nov., an anaerobic, acetogenic bacterium isolated from methanogenic consortia’, *International Journal of Systematic and Evolutionary Microbiology*, 64(Pt_12), pp. 4027–4032. Available at: https://doi.org/10.1099/IJS.0.062711-0/CITE/REFWORKS.

Sasi Jyothsna, T.S. *et al.* (2016) ‘Paraclostridium benzoelyticum gen. nov., sp. nov., isolated from marine sediment and reclassification of Clostridium bifermentans as Paraclostridium bifermentans comb. nov. Proposal of a new genus Paeniclostridium gen. nov. to accommodate Clostridium sordellii and Clostridium ghonii’, *International Journal of Systematic and Evolutionary Microbiology*, 66(3), pp. 1268–1274. Available at: https://doi.org/10.1099/IJSEM.0.000874/CITE/REFWORKS.

Stanley, S.O. and Morita, R.Y. (1968) ‘Salinity effect on the maximal growth temperature of some bacteria isolated from marine enviroments’, *Journal of bacteriology*, 95(1), pp. 169–173. Available at: https://doi.org/10.1128/JB.95.1.169-173.1968.

Strobel, G., Hagemann, B., *et al.* (2023) ‘Coupled model for microbial growth and phase mass transfer in pressurized batch reactors in the context of underground hydrogen storage’, *Frontiers in Microbiology*, 14, p. 1150102. Available at: https://doi.org/10.3389/FMICB.2023.1150102/BIBTEX.

Strobel, G., Zawallich, J., *et al.* (2023) ‘Experimental and numerical investigation of microbial growth in two-phase saturated porous media at the pore-scale’, *Sustainable Energy & Fuels*, 7(16), pp. 3939–3948. Available at: https://doi.org/10.1039/D3SE00037K.

Tarasov, A.L. *et al.* (2011) ‘Isolation and investigation of anaerobic microorganisms involved in methanol transformation in an underground gas storage facility’, *Microbiology*, 80(2), pp. 172–179. Available at: https://doi.org/10.1134/S0026261711020147/METRICS.

Taylor, S. *et al.* (2010) ‘A practical approach to RT-qPCR—Publishing data that conform to the MIQE guidelines’, *Methods*, 50(4), pp. S1–S5. Available at: https://doi.org/10.1016/J.YMETH.2010.01.005.

Thaysen, E.M. *et al.* (2023) ‘Microbial risk assessment for underground hydrogen storage in porous rocks’, *Fuel*, 352, p. 128852. Available at: https://doi.org/10.1016/J.FUEL.2023.128852.

Unfccc (2015) ‘ADOPTION OF THE PARIS AGREEMENT - Paris Agreement text English’.

UNITE (no date). Available at: https://unite.ut.ee/ (Accessed: 11 July 2024).

Vandieken, V. *et al.* (2017) ‘Marinisporobacter balticus gen. Nov., sp. nov., desulfosporosinus nitroreducens sp. nov. and desulfosporosinus fructosivorans sp. nov., new spore-forming bacteria isolated from subsurface sediments of the Baltic Sea’, *International Journal of Systematic and Evolutionary Microbiology*, 67(6), pp. 1887–1893. Available at: https://doi.org/10.1099/IJSEM.0.001883/CITE/REFWORKS.

Watanapokasin, R.Y. *et al.* (2009) 'Hydrogen production and anaerobic decolorization of wastewater containing Reactive Blue 4 by a bacterial consortium of Salmonella subterranea and Paenibacillus polymyxa', *Biodegradation*, 20(3), pp. 411–418. Available at: https://doi.org/10.1007/S10532-008-9232-0/METRICS.

Wishart, D.S. *et al.* (2023) 'MiMeDB: the Human Microbial Metabolome Database', *Nucleic Acids Research*, 51(1 D), pp. D611–D620. Available at: https://doi.org/10.1093/nar/gkac868.

Yoon, S.H. *et al.* (2017) 'Introducing EzBioCloud: A taxonomically united database of 16S rRNA gene sequences and whole-genome assemblies', *International Journal of Systematic and Evolutionary Microbiology*, 67(5), pp. 1613–1617. Available at: https://doi.org/10.1099/IJSEM.0.001755/CITE/REFWORKS

Ahmadpour, S. (2022). Hydrogen Co-Storage with CO_2 in Depleted Gas Reservoirs: Challenges and Opportunities. University of Stavanger, Faculty of Science and Technology, Stavanger, Norway.

Beckman, K.L., Determeyer, P.L. & Mowrey, E.H. (1995). Natural Gas Storage: Historical Development and Expected Evolution: December 1994-February 1995. GRI-95/0214. *Gas Research Institute*, Houston, TX, June 1995.

Flemisch, B., Darcis, M., Erbertseder, K., Faigle, B., Lauser, A., Mosthaf, K., Müthing, S., Nuske, P., Tatomir, A., Wolff, M., & Helmig, R. (2011). DuMux: DUNE for multi-{phase, component, scale, physics,...} flow and transport in porous media. *Advances in Water Resources*, *34*(9), 1102-1112. https://doi.org/10.1016/j.advwatres.2011.03.007

Heinemann, N., Alcalde, J., Miocic, J. M., Hangx, S. J. T., Kallmeyer, J., Ostertag-Henning, C., Hassanpouryouzband, A., Thaysen, E. M., Strobel, G. J., Schmidt-Hattenberger, C., Edlmann, K., Wilkinson, M., Bentham, M., & Haszeldine, R. S. (2021). Enabling large-scale hydrogen storage in porous media – The scientific challenges. *Energy & Environmental Science*, *14*(2), 853-864. https://doi.org/10.1039/D0EE03536J

Henderson, A. (2007). ParaView Guide, A Parallel Visualization Application. Kitware Inc. https://www.paraview.org/

Hogeweg, S., Strobel, G. & Hagemann, B. (2022). Benchmark study for the simulation of Underground Hydrogen Storage operations. *Comput Geosci* **26**, 1367–1378. https://doi.org/10.1007/s10596-022-10163-5

International Energy Agency (IEA). (2021). *Global Hydrogen Review 2021*. Paris: IEA. **https://www.iea.org/reports/global-hydrogen-review-2021**

Kopal, L. ČížekJ, P. & Milicka, J. (2016). Geological model of Lobodice underground gas storage facility based on 3D seismic interpretation. *Contributions to Geophysics and Geodesy*, *46*(2), 125-135. https://doi.org/10.1515/congeo-2016-0009

Lord, A. S., Kobos, P. H., & Borns, D. J. (2014). Geologic storage of hydrogen: Scaling up to meet city transportation demands. *International Journal of Hydrogen Energy*, *39*(28), 15570-15582. https://doi.org/10.1016/j.ijhydene.2014.07.121

Lyu, Z. & Whitman, W.B. (2019). Transplanting the pathway engineering toolbox to methanogens. *Current Opinion in Biotechnology*, 59, 151-157. https://doi.org/10.1016/j.copbio.2019.02.009

Tarkowski R. Underground hydrogen storage: characteristics and prospects. Renew Sustain Energy Rev 2019;105:86e94.

Thaysen, E. M., McMahon, S., Strobel, G. J., Butler, I. B., Ngwenya, B. T., Heinemann, N., Wilkinson, M., Hassanpouryouzband, A., McDermott, C. I., & Edlmann, K. (2021). Estimating microbial growth and hydrogen consumption in hydrogen storage in porous media. *Renewable and Sustainable Energy Reviews, 151*, 111481. https://doi.org/10.1016/j.rser.2021.111481

Tremosa, J. Jakobsen, R. & Le Gallo, Y. (2023). Assessing and modeling hydrogen reactivity in underground hydrogen storage: A review and models simulating the Lobodice town gas storage. *Front. Energy Res.* 11:1145978. https://doi.org/10.3389/fenrg.2023.1145978